Effect of Hydrodynamic Forces on Spanning Pipes

Pakhshan Ahmadian

Submitted to the
Institute of Graduate Studies and Research
in partial fulfillment of the requirements for the Degree of

Master of Science
in
Civil Engineering

Eastern Mediterranean University
July 2015
Gazimağusa, North Cyprus

Approval of the Institute of Graduate Studies and Research

Prof. Dr. Serhan Çiftçioğlu
Acting Director

I certify that this thesis satisfies the requirements as a thesis for the degree of Master of Science in Civil Engineering.

Prof. Dr. Özgür Eren
Chair, Department of Civil Engineering

We certify that we have read this thesis and that in our opinion it is fully adequate in scope and quality as a thesis for the degree of Master of Science in Civil Engineering.

Assoc. Prof. Dr. Umut Türker
Supervisor

Examining Committee

1. Assoc. Prof. Dr. Umut TÜRKER

2. Assoc. Prof. Dr. İbrahim YİTMEN

3. Asst. Prof. Dr .Serhan ŞENSOY

ABSTRACT

In this study the spanning behavior of submerged pipes are analyzed and discussed. In the order to do so the limits of Reynolds number less than 3.5×10^5 and Keulegan Carpenter number is between 4 and 7acsepted as limitation of the work. Under this limitation it is clear that even at low orbital velocities momentum initiates at intermediate depth. Therefore the current velocity and orbital velocity at intermediate depth are computed to determine the in-line and cross-flow net forces on spanning submarine pipe. These forces were useful while calculating the maximum deflections and moment that occurs at the mid length of the pin supported pipes. The magnitude of yield stress of HDPE pipes are then compared with the maximum bending stress of the pipe in the order to calculate the critical spanning length of different HDPE pipe diameter and thicknesses. The results show similarity with the model which was generated for spanning steel pipes. This deflection calculated for simply support pipes and also modelled in the ANSYS software.

Keywords: Vortex, Drag force, Inertia force, HDPE, Span length.

ÖZ

Bu çalışmada batık borular üzerine gelen yayılı yüklerin boru davranışına yaptığı etkinin analizi yapılmış ve tartışılmıştır. Çalışmanın limitasyonu Reynolds sayısının 3.5 x 10^5'den küçük ve Keulegan Carpenter numarasının 4 ve 7 arasında sınırlandırılmasını öngörmektedir. Bu sınırlar içerisinde dalgadan dolayı oluşmakta olan yörüngesel hızların boru etrafındaki momentum hareketlerini aktive ettiği bilinmektedir. Bu nedenle orta derinlikteki batık boruların üzerine etki eden akıntı hızları ve yörünge hızı boruya dik ve boru boyunca hesaplanmış ve hızların yarattığı tüm kuvvetler tanımlanmıştır. Boruya dik ve paralel etki eden kuvvetler borunun orta noktasında maksimum deplasmanları oluşturmuş ve bu kuvvetlerin bir çift vortex oluşumuna olanak sağladığı gözlenmiştir. HDPE borularda maksimum momentlerin yarattığı gerilmeler borunun akma gerilmesi ile karşılaştırılmış ve altı oyulan askıdaki boruların maksimum askı uzunluğu hesaplanmıştır. Sonuçlar çelik boruları kapsayan daha önce türetilmiş denklemlerle karşılaştırılmıştır. Her iki sonuçlar da birbirleri arasında benzerlik göstermişlerdir. Ayni samanda borularda oluşan deplasmanlar ANSYS yazılımı ile modellenmiş ve sonuçlar bilindik denklem ile karşılaştırılmıştır.

Anahtar Kelimeler: Vortex, Sürükle kuvveti, Atalet kuvveti, HDPE, Span uzunluğu

ACKNOWLEDGEMENT

I would like to express my deepest and heartfelt appreciation to my supervisor Dr.Umut Turker who gave me the motivation, kindness help to complete this thesis. And his guidance which have been a remarkable help during the work process. Moreover I would like to convey my special thanks to examining committee members, especially Asst.Prof.Dr, Serhan Sensoy for his effect in evaluating my study.

I would also like to thank myself as trusted and believed in myself despite all hardship.

My sincere appreciation goes to my family members specially my parents who have made their support for me and were patient with me all throughout this research my husband, Chia mahammad jani, who helped me to complete through my thesis process.

LIST OF CONTENT

LIST OF FIGURES

LIST OF TABELS

LIST OF SYMBOLS/ABBREVIATION

CF	Cross flow
FEM	Finite element method
IL	In line flow
MRS	Minimum requested strength
Re	Reynolds number
VIV	Vortex induced vibration
a_x	Acceleration in horizontal direction (m/sec^2)
C	Boundary condition (dimensionless)
C_a	Added mass coefficient (dimensionless)
C_d	Drag coefficient (dimensionless)
C_L	Lift coefficient (dimensionless)
C_m	Hydrodynamic coefficient (dimensionless)
C_1	Wave celerity in intermediate depth water (m/sec)
C_0	Wave celerity in deep depth water (m/sec)
d	Sea water depth(m)
D_0	Outer pipeline diameter (m)
D_I	Internal pipeline diameter (m)
E	Elastic modulus (N/m^2)
F_B	Buoyant force (N)
F_D	Drag force (N)
F_{hyd}	Inertia force or hydrodynamic mass (N)
F_L	Lift force (N)
f_n	Natural frequency (Hz)

F_P	Froude krylov force (N)
f_{VIV}	Vortex induced vibration frequency (Hz)
Fy	Yield stress (N/m2)
H	wave height (m)
H_{new}	New wave height (m)
I_x	Area moment of inertia (m^4)
KC	Keulegan-Carpenter number for oscillatory flow
K_S	shoaling coefficient (dimensionless)
L	Span beam length (m)
L_P	Pipe Span length (m)
M	Bending moment (N. m)
m	Mass (kg)
m_T	Total mass (kg)
Re	Reynolds number (dimensionless)
S	Bending stress (N/m^2)
St	Strouhal number
t	Wall thickness of pipe (m)
T	Wave period (sec)
Uc	Current velocity (m/sec^2)
U_T	Total velocity (m/sec^2)
U_x	Horizontal orbital velocity (m/sec)
U_Z	Velocity at a depth z (m/sec^2)
U_v	Vertical particle velocity (m/sec)
V_r	Reduced velocity of pipe
W_C	Pipe content weight (N)

W_A	Pipe water displacement weight or weight of added mass (N)
W_P	Pipe weight (N)
W_T	Total mass (N)
y_x	Pipe deflection at point x (m)
y	Pipe deflection (m)
z	Reference elevation (m)
ʎ	Wave length (m)
v	Volume of cylinder (m^3)
g	Acceleration of gravity (m/sec^2)
α	Angle of current direction (degree)
θ	Angel between wave and pipe (degree)
ρ	Density (kg/m3)
δ	Stress (N)
ν	Kinematic viscosity (m2/se

Chapter 1

INTRODUCTION

1-1 Literature Review

Before initiating a research study it is necessary to understand and summaries what has been done on that area by others in pervious researches. For sure, a series of different codes were used and several papers were published. Some of these outstanding codes which most of analyses were based on basic hydrodynamic theories are as following.

In order to understand the physics of the environmental conditions and environmental loads for submarine pipes, the Det Norske Veritas (DNV-RP-C205) [8] was used. This Recommended Practice (RP) provides regulation for modelling, analysis and forecast of environmental circumstances plus assistance for calculating environmental loads performing on structures. The loads are limited to those due to wind, wave and current. The RP is following an artistic manner throughout modelling and analysis of environmental situations and loads and applied developments in recent research and development assignments, as well as design knowledge from fresh projects.

A part of submarine pipe investigated in this study is supposed to function as a free span pipeline owing to the irregularities of sea bed resulting from settlements of the sea floor or erosion of the seafloor due to currents around the pipes. For such conditions, the proposed guidelines for design procedures are the DNV-OS-F101[1], DNV-RP-F105[2], BS 8010 (BS, part 3, 1993) [3] and most valuable one which is directly dealing with the rules for submarine pipeline, DNV 1981[4]. Most of the rules and equations allocated during the analysis were mainly from this latest code. The main focus of DNV 1981 [4] is to investigate the rules requirement for stability of free suspended pipe. A comprehensive number of graphs are presented in this standard to assess the important of in-line and cross-flow section potential of pipes for checking vortex shedding occurrence.

Different studies have been done on flow field around submarine pipeline and they are investigated for several waves, free surface, bottom boundary, water depth and marine growth behaviors. Among them Zhi-Peng Zang et.al [12] simulated the effect of wave height on wave force on submarine pipeline with finite volume method using two-dimensional Navier–Stokes equations. They compare the theoretical findings with experimental results and finally he concluded that the horizontal wave force varies relatively linear with the wave height and found that the effect of seabed on horizontal wave forces is not remarkable. In addition they found that when the gap ratio is bigger than 0.5 the drag coefficient and inertia coefficient are constant.

Muk Chen Ong et.al [13] in 2004 had investigation about high Reynolds number flows around a circular cylinder near to a flat seabed with using the k–ε model with different gap ratio. In this study they focused on high Reynolds number flows regime at $Re=3.6\times10^6$ with different gap ratio by using the numerical simulation. As a result they found that if the gap ratio is equal to 1, the sea bed has no effect on the formation of vortex shedding around cylinder as can see in Figure (1.1).

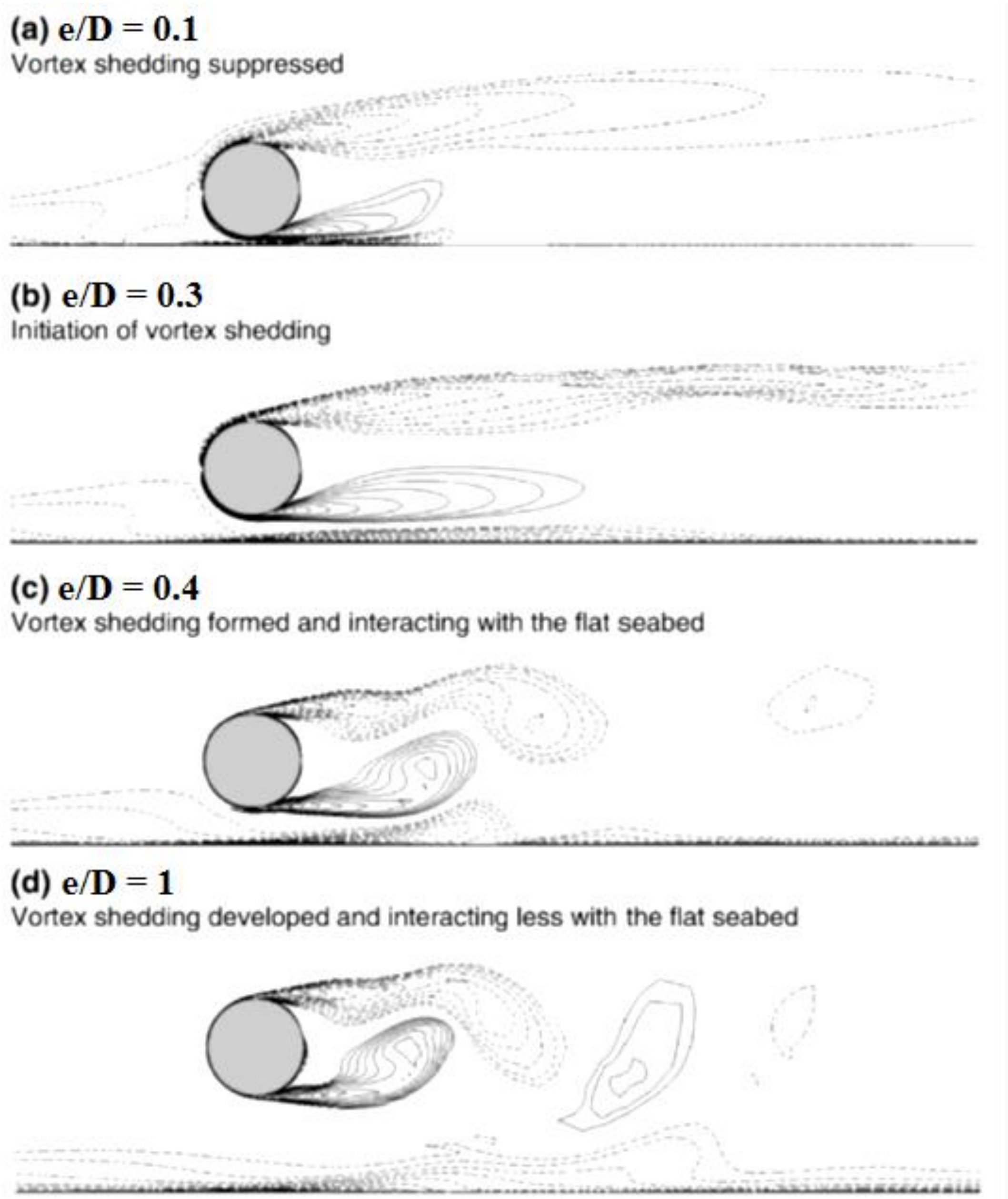

Figure 1.1: Flow around a circular cylinder for Re=1.31×104 and [13]

Several researchers have found interesting results on submerged pipeline with different material properties, especially for steel material. Among them we can refer to Choi (2000) [14]. In his study he found that the substantial effect of axial forces on natural frequency (Figure 1.2) and free span length analysis (Figure 1.3). In his research he compared several boundary conditions such as fix-fix, pip-pin, and fix-pin, fix-free and used the DNV codes to modify the allowable span length for steel pipe. He found that during the operation and installation the allowable span lengths start to increase with an increment in tension, and decrease with an increment in compression.

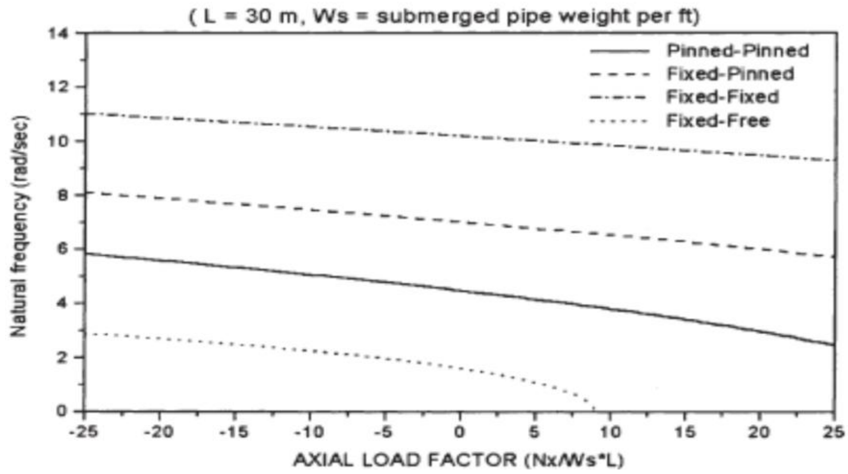

Figure1.2: Effect axial forces on natural frequency [14]

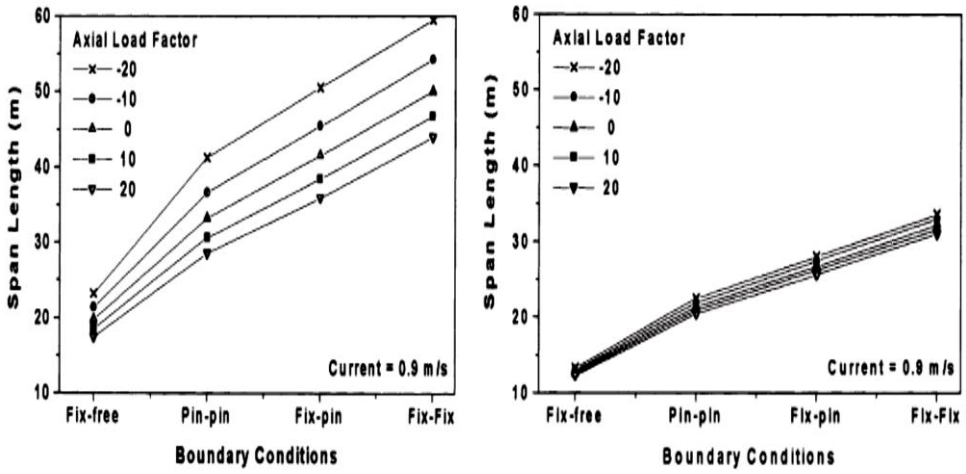

Figure 1.3: Allowable span length with axial forces in crass-flow and in-line flow[14]

Rita G. Toscano et.al [15] did a research about experimental validation of a finite element model that simulates the collapse and post-collapse behavior of steel pipes. They compered the numerical and experimental results of three samples with different thickness and outer diameters under external pressure without bending for steel pipes.

Sumer and Fredsoe, carry out detailed analyses on submarine pipes and calculated their result as a book [5]. They focused on hydrodynamic around cylindrical structure in which both orbital velocity and normal velocity components were taken into consideration. In their result it was clear that vortex induced vibration, (VIV), due to spanning of pipes were occurring when KC was greater than 7. They have found that when KC is between 4 and 7 a pair of vortex occurs around the pipe. When a pair of vortex is in action the pipe behaviors will be linearly and no damping occurs due to hydrodynamic forces. However, even in that mode still deformation occur on the pipe and failure is expected for long spanning length. Yet there are no studies focusing on HDPE pipes and checking the failure modes when pair of vortex occurs around the spanning submarine pipes. Therefore in this study hydrodynamic forces on HDPE spanning subsea pipes will be analyses and the failure limits will be stated.

Havar A. Sollund et.al [29], did a research on semi-analytical method for multi-spans by allocating the finite element models. The aim of this method was focusing on effects of axial forces and elementary curvatures due to static deformations. They used several codes such as DNV-OS-F101 and DNV 1981 for their studies and approved that for computing the dynamic response of multi-span pipelines, novel semi-analytical method should be modified by finite analyzing methods. In addition they concluded that the in-line and cross-flow fundamental frequencies may undertake a considerable decrease due to attendance of neighboring spans. In-line modal stresses will steadily descent, while cross-flow modal stresses will rise or decline.

Z.C. Zheng et.al [30], focused on investigating frequency range due to effects on drag and lift forces around oscillating cylinder and discussed about time history on them. In this research, the simulations of unsteady fluid dynamic are realized. They studied three cases of fundamental frequency and oscillation frequencies close and away from the natural frequency. They proved that in same case when there is a coupling between the oscillations and the natural vortex shedding, high range of C_L and C_D are observed. Consequently By going away from natural frequency, frequency of vortex shedding will be observe for lift and drag forces.

Abbas Yeganeh et.al [31], investigated the independent parameters to influence of Varity sea bed deformation on natural frequency. The basic of this assessment, evaluated the allowable free span length for steel pipes by using the modal analysis in Gheshm Island. They noticed that the axial forces have significant effect on evaluating the allowable free span length for steel pipe. In addition they concluded that only for a pipe with both end fixed supports, axial force can be ignored otherwise for other supports like pinned connections, the effect of this axial forces has important role for allowable free span pipe evaluation.

1-2 Definition of a Problem

A marine pipeline designed at the bottom of the sea bed is generally accepted to be stable since the anchored blocks positioned at a predefined and calculated intervals are strong enough to attain the stability and the underlying soil is capable to withstand the weight and the hydrodynamic forces in the system. However, the idealized behavior of pipeline to be in contact with a stable seabed throughout its lifetime sometimes fails. This failure is generally due to the settlements of the sea floor or erosion of the seafloor due to currents around the pipes. This separation of the sea bed from the surface of the pipeline generates suspended spanning lengths at the sub sea. Free spans sometimes occur due to the irregularities of the sea bed. In such case depending on the length of the span, lift forces, inline forces and the properties of the pipeline, significant deflections occurs that disturbs the natural frequency of the pipelines. The behavior of free spanning pipes has been defined and set out in various codes and standards ([1],[2],[3],[4]) and also defined in detailed in a broad collection of books and papers ([5],[6],[7]). Most of these studies are focused on the analyses of vortex induced vibrations at spanning lengths for steel pipes in which Keulegan Carpenter number is greater than seven, at high Reynolds numbers and the pipe is located at the shallow water depths. However, at intermediate depths, the oscillatory effects of the sea waves are still dominating the hydrodynamic forces and failure of the pipeline is still possible due to the hydrodynamic forces and changes in the natural frequency of the pipes.

In this thesis, attempts have been made to investigate the natural frequency of free spanning HDPE pipes under the influence of hydrodynamic forces. The main aim of choosing HDPE pipes are made of very flexible material, therefore their installations process in submarine could be much simpler than other kind of pipelines material. In this regard, various boundary conditions, Reynolds Number less than 3.5×10^5 and Keulegan Carpenter number in between 4 and 7 were considered and the results were analyzed.

1-3 The Study Context

This study is conducted at Eastern Mediterranean University. The tools used in this study are the ANSYS software, MATLAB software and the computer laboratory of the Civil Engineering Department. All the theoretical calculations related with the hydrodynamic calculations are carried out by the help of MATLAB software in which a code is developed.

1-4 Research Questions

The research is based on the following questions:

1. What is the effect of lift forces on the behavior of spanning pipes?
2. What is the effect of inline forces on the behavior of spanning pipes?
3. What is the relationship between the dimensionless forces parameter and the dimensionless depth parameter?
4. What is the relationship between the dimensionless forces parameter and the dimensionless diameter parameter?
5. What is the effect of total net forces on free spanning pipe length by different diameters and thicknesses?
6. What is the effect of total net forces on free spanning pipe deflection by different diameters and thicknesses?

1-5 Aims and Objectives of the Research

The main goal of this study is to quantify the magnitude of hydrodynamic forces such as uplift force and inline force, exerted on the spanning HDPE pipes during the failure at predefined Reynolds and Keulegan Carpenter numbers. The deflections in the spanning pipes are usually due to these forces. The deflection in the pipe changes the normal frequency of the pipes which can be the reasons of any failure. These forces are usually generating vortex induced vibrations around the pipes specially in shallow water conditions since the orbital velocity of the waves are high. High orbital velocity generates high Reynolds Numbers and high Keulegan-Carpenter numbers which are the main reasons of vortex induced vibrations that are dominating the behavior of the pipes and increases the risk of failure. However, as the pipe goes deeper, such as intermediate depth, the orbital velocity decreases, lowering the magnitudes of Reynolds number and Keulegan-Carpenter number. In such cases, vortex induced vibration is not effective, but the risk of failure is still ongoing since pair of vortex is still present. Such an environment is possible at intermediate depth at low Reynolds and Keulegan-Carpenter number.

1-6 The Proposed Methodology

The requirement of the study was to extract reliable, accurate and physically possible results. Therefore, the main methodology of the study was proposed as a quantitative research. Quantitative analysis was helpful while approaching the results since the previous studies, standards and references were valuable and well organized while guiding the physical behavior of spanning submerged pipelines.

The methodology followed was initiated by finding the interval in which the limitations of pair of vortex around the spanning pipe starts. This was achieved at intermediate zone where due to the small effects of orbital velocity of the waves, the Reynolds Number and Keulegan-Carpenter number are small. Later, the ratio between the inline forces and lift forces are examined. This was necessary to understand at which conditions vortex induced vibration dominates due to inline forces and at which level a pair of vortex occurs where lift forces are dominant. As long as the required limitations were dominating the flow characteristics the natural frequency of the pipes are compared with the vortex shedding frequency of the pipes. Finally, the results of the analyses, failure limits of HDPE pipes, and the corresponding maximum possible span lengths are evaluated, plotted, analyzed and discussed.

1-7 Limitations of the Study

The limitations of the study were necessary in order to have clear boundaries in the definition of the problem. It was obvious that the subcritical flow conditions must be pervading around the pipe in order to have only a pair of vortex around the pipe. This can only be achieved when flow Reynolds Number is below 3.5×10^5 and Keulegan-

Carpenter number is in between 4 and 7. Therefore, during the study these two criteria were always checked. These limitations were only valid at intermediate depths. Also, in this study it is always accepted that the diameter of the pipe is small related to the wave length considered. The ratio of diameter to the wavelength considered was around $0.006 < D/\lambda < 0.008$.

1-8 Outline of the Study

The thesis consists of five different chapters. First chapter aims to give a short introduction to the research while defining the problem statement, aims, objectives and methodology of the study. The second chapter briefly explains the fundamentals of the water sea wave hydraulics loading, hydrodynamic forces and behavior of submerged pipes. Chapter 3 is focused on the environmental loading and total in-line forces and cross-flow forces, the results of this studies is define by means of figures, tables, drawings and explanations . Chapter 4 gives discussions about the effect of these total forces on free spanning pipe length and deflection with different thicknesses and diameters by means of figures, tables, drawings and explanations. Final chapter, Chapter 5 gives conclusions and recommendations for future studies.

Chapter 2

FUNDAMENTALS OF HYDRODYNAMIC FORCES

2.1 Overview

In this chapter the fundamental of costal engineering and hydrodynamic forces on submarine pipes will be presented. At first step the theories and descriptions about the environmental conditions of coastal regions in intermediate depth conditions are presented. In the next step formulas for stability of suspended pipe and hydrodynamic forces around cylinder pipes in in-line and cross-flow section regarding the relevant codes is clarified. Finally, comprehensive information about the polyethylene material and the structural behavior of pipelines made of polyethylene material is investigated when both the end connections are simply supported.

2.2 linear wave theory

2.2.1 Basic Assumptions and Definitions

There are a lot of theoretical descriptions of waves, the EM 1110-2-1100 [16] wave codes was used for definitions of these theoretical descriptions. The most elementary of them are the small-amplitude or linear wave theory. On the other hand Dean and Dalrymple 1991[33] described waves by higher-order theories which called as finite-amplitude wave theories. There are some assumptions in applying of linear wave theory which are [16]:

- Thorough of application the density ρ, is a constant which means that the flow is incompressible.
- Surface tension is ignored.
- The flow is irrotational.
- The fluid is inviscid.
- The wave amplitude is small and it is consistent in time and space.

2.2.2 Flow velocities and accelerations

Whenever the depth of the sea, d, is between the wavelengths $\frac{\lambda}{2}$ and $\frac{\lambda}{20}$ the approaching wave's transitional water conditions are dominating the environmental forces at subsea region. The valid limitation of transitional water condition is given in shore protection manual as:

$$\frac{\lambda}{20} < d < \frac{\lambda}{2} \tag{2.1}$$

At this depth, If T is wave period and g is gravitational accretion the wavelength can be approximated by [16]:

$$\lambda = \frac{g}{2\pi} T^2 [\sqrt{\tanh \frac{4\pi^2 d}{gT^2}}] \tag{2.2}$$

It is very well known that any wave with length ʎ, height H and wave period T at a water depth d creates horizontal and vertical water particle velocity defined as:

$$U_x = \frac{TgH}{2\lambda} \times \frac{\cosh(2\pi(z+d)/\lambda)}{\sinh(2\pi d/\lambda)} \times \cosh\left[\frac{2\pi x}{\lambda} - \frac{2\pi t}{T}\right] \tag{2.3}$$

$$U_y = \frac{TgH}{2\lambda} \times \frac{\cosh(2\pi(z+d)/\lambda)}{\sinh(2\pi d/\lambda)} \times \sinh\left[\frac{2\pi x}{\lambda} - \frac{2\pi t}{T}\right] \tag{2.4}$$

In which x is horizontal and z is vertical point in fluid in the velocity vector. The horizontal water particle velocity is normally results to the formation of drag and lift forces. Alternatively inertia forces will be induced by relevant water particle acceleration in the horizontal direction. The acceleration is defined as:

$$a_x = \frac{g\pi H}{\lambda} \times \frac{\cosh(2\pi(z+d)/\lambda)}{\sinh(2\pi d/\lambda)} \times \sinh\left[\frac{2\pi x}{\lambda} - \frac{2\pi t}{T}\right] \tag{2.5}$$

Usually the scale of vertical and horizontal velocities decreases as the depth of subsea increases. Their effect can be ignored when deep water conditions are leading the environmental condition. In any case, the horizontal water particle velocity and horizontal acceleration at transitional water conditions according of EM 1110-2-1100 [16] can be simplified into:

$$U_x = \frac{TgH}{2\lambda} \times \frac{\cosh(2\pi(z+d)/\lambda)}{\sinh(2\pi d/\lambda)} \times \cosh\theta \tag{2.6}$$

$$a_x = \frac{g\pi H}{\lambda} \times \frac{\cosh(2\pi(z+d)/\lambda)}{\sinh(2\pi d/\lambda)} \times \sinh\theta \tag{2.7}$$

With the phase angel, $\theta = 2\pi(\frac{x}{L} - \frac{t}{T})$.

2.2.3 Current velocity

It is approved that tides have different depths which results from landscape alterations. All decent and assents variations affects the current velocity. To assess the tidal currents, the one-seventh power law is used. The current speed is even related to the wind coming from different directions. The wind makes speed variations which has a linear equation with the tidal speed. This variation is specified as a maximum speed at the upper surface of the water and as zero speed at the bottom, Modeling Coastal and Offshore Processes book [17].

The equation 2.8 represents that power law in costal and offshore engineering as a function of depth in the lower half of the flow.

$$U_c = U_z (\frac{d}{z})^{\alpha} \tag{2.8}$$

Which in U_z is velocity in the depth z, d is the depth of seawater and α is a coefficient where it dependents to the stability of the environmental, for natural stability it is approximately 1/7, or 0.143 in offshore structure.

2.3 Forces on a pipe in regular waves

2.3.1 Basic concept

A pipe subject to an oscillatory flow experiences two kinds of forces namely in-line force and the cross flow forces (Figure 2.1). In the following, first, the in-line force will be considered which is the resultant horizontal force acting on a submerged cylindrical pipe and second, the vertical cross flow forces will be discussed that deflects the pipes in vertical direction.

2.3.2 Inline forces

In steady open channel flows or currents the force that acts on different cylindrical shapes in the inline direction is generally defined as inline force (drag force) and it is given by

$$F_D = \frac{1}{2} \rho C_D \rho U^2 \tag{2.9}$$

Where F_D is the force per unit length of the cylindrical shape and C_D is the drag coefficient. The ρ is the density of the fluid and U represents the flow velocity (summation of the wave orbital velocity and current velocity in the case of oscillatory flow). On the other hand, whenever the steady open channel flow is converted into oscillatory flows, two other forces are added up to the above total in line force [5].

$$F_I = \frac{1}{2} \rho C_D \rho U^2 + m' \dot{U} + \rho V \dot{U} \tag{2.10}$$

In which $m'\dot{U}$ represents the hydrodynamic mass force and $\rho V\dot{U}$ is called the Froude – Krylov force. In Equation (2.10) m' represents the hydrodynamic mass and *V* represents the volume of the cylinder shape (pipe) [5]. As long as the total in line force calculations are carried out for a unit length of a cylindrical shape the volume term in Froude – Krylov force reduces into cross sectional area, *A*.

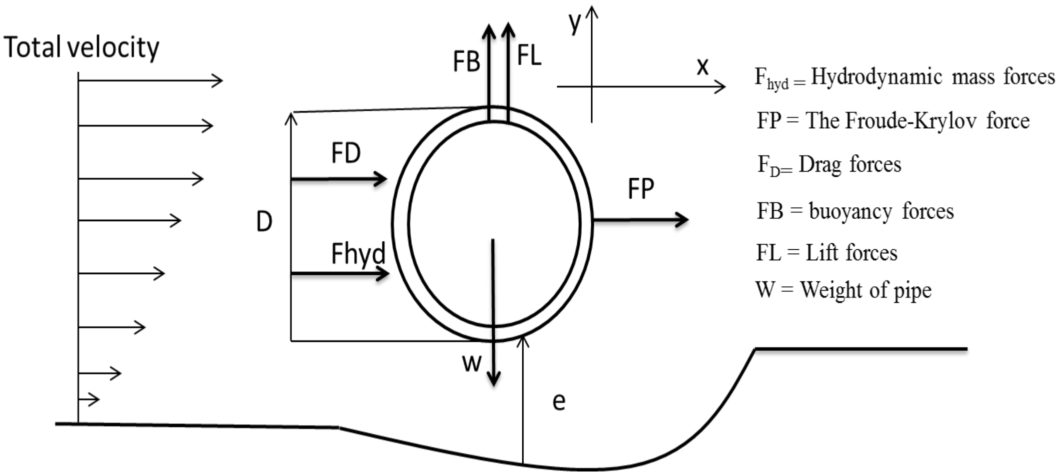

Figure 2.1: Sketch map of forces acting on the submerged pipe

2.3.2.1 Hydrodynamic mass forces (F_{hyd})

The hydrodynamic mass is the accelerated mass of the fluid around a cylindrical body due to the motion of the body towards the fluid. If this motion easily splits into fluid the effect of added mass is small. Otherwise, the magnitude of the hydrodynamic force of a circular cylinder can be given as while applying pressure on the fluid defined as the mass of the fluid around the body which is accelerated with the movement of the body due to the action of pressure [5].

The hydrodynamic mass of a circular cylinder is given as [5]:

$$m' = \rho\pi r^2 \tag{2.11}$$

in which r is the radius of the pipe and thus πr^2 is the cross sectional area of the pipe. Inserting the area term into equation (2.11) the hydrodynamic mass equation can be written as [5]:

$$m' = \rho c_m A \qquad (2.12)$$

The coefficient c_m in the above equation is known as hydrodynamic mass coefficient and for cylindrical pipes it can be accepted to be equal to one. The magnitude of hydrodynamic mass increases as the gap ratio between the cylinder and the bed decreases. This can be observed from Figure 2.2 (Yamamoto et al. (1974).

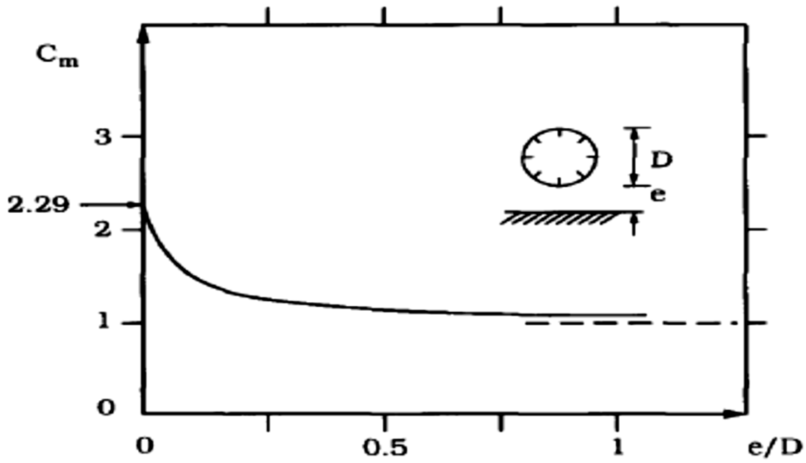

Figure 2.2: Hydrodynamic-mass coefficient for a circular cylinder near a wall [5]

2.3.2.2 The Froude-Krylov force (F_P)

The hydrodynamic mass force is a force on the body of water when the body is moved with acceleration in still water. As mentioned before this force is directly caused by the acceleration of the fluid in the immediate surroundings of the submerged body [5]. On the other hand, when there is an acceleration of fluid in the immediate surroundings (outer-flow region) of the body another force will occur due to the pressure gradient. This pressure gradient generates additional forces on the cylinder which is named as Froude-Krylov force. This force which is due to the pressure gradient on the cylinder is given as [5]:

$$F_p = \rho A\dot{U} \tag{2.13}$$

It is necessary to note that the Froude-Krylov force is due to the pressure gradient of moving fluid. Therefore, for those bodies which are submerged in still water Froude-Krylov force does not exist.

2.3.2.3 Morrison equation

With the intention of reducing the failure possibility of subsea pipeline systems stable design conditions should be guaranteed even under the worst case conditions. In order to maintain the stability it is important to delineate the total net in-line force acting on a submerged pipe. This can be achieved by combining two well-known equations; drag in a current and hydrodynamic inertia in an accelerating flow. Superimposing these equations will result in a famous Morrison equation.

$$F_I = \frac{1}{2}\rho C_D \rho U^2 + \rho C_m A\dot{U} + \rho A\dot{U} \tag{2.14}$$

Rearranging the above equation results in

$$F_I = \frac{1}{2}\rho C_D \rho U^2 + \rho\left(C_m + 1\right)A\dot{U} \tag{2.15}$$

Where a new coefficient called Inertia coefficient, C_M can be introduced as being equal to

$$C_M = \left(C_m + 1\right) \tag{2.16}$$

and therefore new force term from the addition of Froude-Krylov force and hydrodynamic force will be generated called as inertia force. The final form of the Morrison equation is therefore can be written as,

$$F_I = \frac{1}{2}\rho C_D \rho U^2 + \rho C_M A\dot{U} \tag{2.17}$$

2.3.3 Forces on a cylinder in cross-flow direction

In general the cross flow forces take place due to the difference in the pressure at the top and bottom of a cylinder. This is due to changing in the velocity of the flow passing the body. The cross flow forces can be summarized as weight of the submerged body, buoyancy force and the lift force [18]. In general, net cross-flow forces causes deflections in the pipe.

2.3.3.1 Buoyancy forces

If an object is submerged in a liquid, or floating on its surface, the net vertical force acting on it due to liquid pressure is termed buoyancy. Consider an object totally immersed in static liquid, as shown in Figure 2.3. The vertical force on the body due to hydrostatic pressure may be found most easily by considering cylindrical volume elements similar to the one shown in Figure 2.3. The pressure *P* at a depth *h* in a liquid can be written as[34],

$$p = p_o + \rho g h \tag{2.18}$$

The net vertical pressure force according to Figure 2.3 on the element is then,

$$dF_z = (p_o + \rho g h_2)dA - (p_o + \rho g h_1)dA = \rho g(h_2 - h_1)dA \tag{2.19}$$

In which the term $(h_2 - h_1)dA$ can be rewritten as the volume of the body given in the figure. Therefore the Equation (2.20) can be written in the following form

$$F_z = \int dF_z = \int_V \rho g dV = \rho g V \tag{2.20}$$

where *V* is the volume of the object. Hence we conclude that for a submerged body the buoyancy force of the fluid is equal to the weight of displaced fluid,

$$F_{buoyancy} = \rho_{liquid} g V_{body\,volume} \tag{2.21}$$

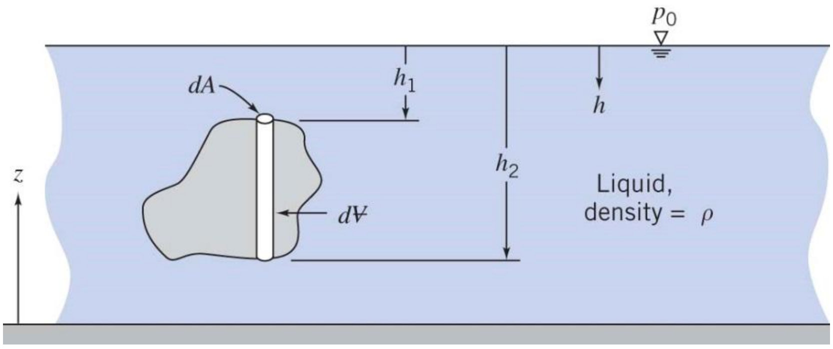

Figure 2.3: Immersed body in static liquid [34]

The line of action of the buoyant force passes through the center of volume of the displaced body. The point which $F_{buoyancy}$ acts is called the center of buoyancy.

2.3.3.2 Weight of submerged bodies

The pipe with weight W_p per unit length can be expressed in terms of pipe specific weight, fluid density, gravitational acceleration and the cross-sectional area of pipe.

$$W_p = SG\rho_{water} gA \tag{2.22}$$

Where SG is the specific gravity; ρ_{water} is the density of pervading fluid, water; g is the gravitational acceleration and A is the pipe cross-sectional area. It is necessary to add the weight of fluid available in the pipe during its operation. The net weight of the pipe is important while deciding on the stability of the submerged pipes.

2.3.3.3 Lift Forces

A submerged cylinder may be under the effects of lift force when it is subjected to oscillatory flow regimes. Lift force is not expected to occur around the cylinder when dimensionless Keulegan-Carpenter (KC) number is very small. The lift force first occurs when KC number is around 4. It is well known that when KC values approaches to 8, vortex induced vibration around the cylinder becomes dominant. In general, for submerged cylinders, lift force generates cross-flow vibrations whereas; drag forces induce in-line vibrations. Nevertheless, whenever KC is greater than 7 these vibrations generate vortex induced vibrations around the submerged cylinders. The lift force is defined as [18]

$$F_L = \frac{1}{2}\rho C_L D U^2 \tag{2.23}$$

Where F_L is the lift force and C_L is the lift force coefficient.

It is very well known that Reynolds number is one of the well-known dimensionless numbers that describes the ratio between the inertia forces and viscous forces in steady currents around submerged cylinders. In those cases where the cylindrical shape is exposed to an oscillatory flow an additional dimensionless number which is a function of orbital velocity, diameter of cylinder and wave period must be considered. This number is called Keulegan-Carpenter number (KC).

Keulegan-Carpenter number is therefore defined by

$$KC = \frac{U_m T}{D} \tag{2.24}$$

in which U_m is the maximum orbital velocity and T is the period of the oscillatory flow. Small KC numbers mean that the orbital motion of the water particles is small relative to the total width of the cylinder. Large KC numbers, on the other hand, mean that the water particles travel quite large distances relative to the total width of the cylinder, probably resulting in vortex shedding.

2.3.3.4 Stability in cross-flow direction

In the case of occurrence of cross-flow forces a subsea pipeline is exposed to unstable behavior. Considering all the forces mentioned before one can easily write the following relationship for the stability of the pipes on the sea floor.

$$W_P = F_B + F_L + NS_U D \tag{2.25}$$

In which N is the bearing capacity factor, S_u is the undrained shear strength and D is the pipe diameter (reference is the journal in 2006 waterway etc.). On the other hand, the term NS_UD drops from the above equation if one is considering the detached position of the pipe from the seafloor and considers the spanning length of the pipe.

$$W_P = F_B + F_L \tag{2.26}$$

If the weight of the pipe is less ($W_P < F_B + F_L$), it means that the pipe will float up and if it is heavy ($W_P > F_B + F_L$) it means that the pipe sinks towards the sea floor. Due to the effect of these forces the pipe dislocates and has cause damage to the pipeline systems, over stressing in case of excessive displacement. Stability is the main concern while ensuring the long term safe operation of pipeline systems. In Figure 2.4 can see the three dimensional stability analysis of combined force due to wave and current velocity [3].

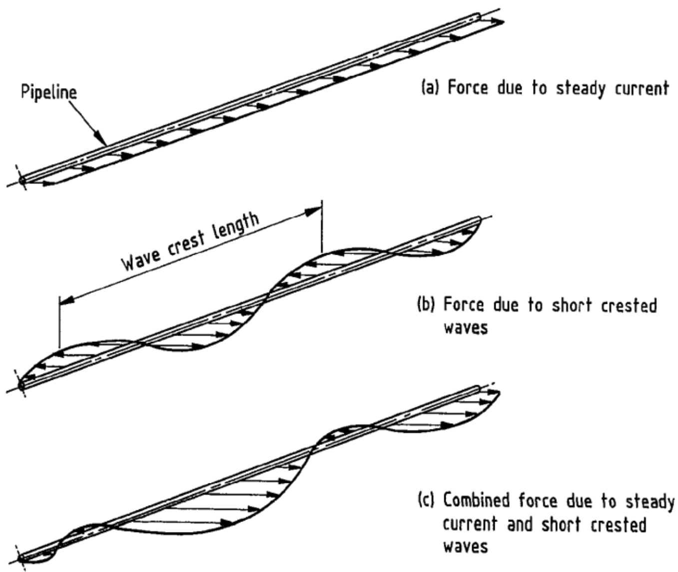

Figure 2.4: three dimensional stability analysis approaches [3]

2.3.4 In-line and cross flow hydrodynamic coefficients

Several coefficients are used in the definition of drag force, lift force, inertia force etc. as given in the previous sections of this thesis. These coefficients can be summarized as the hydrodynamic coefficients, C_D, C_L and C_m. Referring to the Det Norske Veritas (DNV) codes [8], the hydrodynamic coefficient C_D, C_L and C_m are function of Reynolds number as well as the Keulegan-Carpenter number (KC), and the gap (e) between the pipe and seabed. Table 2.1 shows the relationship of hydrodynamic coefficients with the Reynolds [6].

Table 2.1: Recommended coefficient for pipe design

Re	CD	CL	Cm
$Re<5\times10^4$	1.3	1.5	2
$5\times10^4<Re<1\times10^5$	1.2	1	2
$1\times10^5<Re<2.5\times10^5$	$1.53 - (Re/3\times10^5)$	$1.2 - (Re/5\times10^5)$	2
$2.5\times10^5<Re<5\times10^5$	0.7	0.7	$2.5 - (Re/5\times10^5)$
$5\times10^5<Re$	0.7	0.7	1.5

2.4 Vortex Shedding

As soon as low pressure zones (blue color in Figure 2.5) initiates downstream of a circular boundary, KC approaches to 8 and vortex shedding is generated. These low pressure zones forces the circular boundary to move towards the low pressure zone, generating displacement of circular boundary perpendicular to the direction of the flow. When the vertical, critical speed of circular boundary is reached the circular boundary resonate where large forces and deflections are experienced. As the vibrations of circular boundary enlarge vortex shedding occurs that lead to damage and may create failure without exceeding the ultimate limit stress.

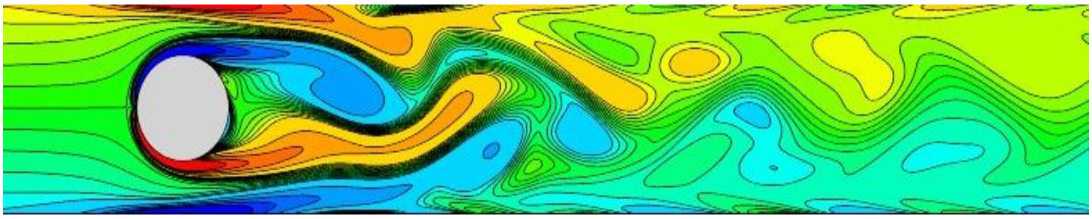

Figure 2.5: Vortex shedding phenomenon induced by flow around a circular boundary.

Vortex induced vibration occurs due to the vortex shedding occurrences both in in-line and cross-shore directions.

2.4.1 In- Line Vortex Shedding

In the In-line direction the spanning pipe starts to oscillate when the vortex shedding frequency of a pipe is approximately one-third times of the natural frequency [4]. In-line oscillations are excited at flow velocities lower than the critical velocities for cross-flow motion. However, the amplitude of the in-line motion is only 10% of those associated with cross-flow motion. Natural frequency of the spanning pipe depends to length of pipe, total mass of pipe (addition of mass of pipe, mass of fluid content and add mass around the pipe) and end condition of spanning pipe as given below:

$$f_n = \frac{C}{L^2}\left(\sqrt{\frac{EI}{m}}\right) \tag{2.27}$$

Where *C* depends to the type of supports at both ends of the pipe [7], as given in Table 2.2; L is the pipe spanning length; E is the modules of elasticity; I is the moment of inertia and *m* is the total mass.

Table 2.2: Classification of *C* depending on the end condition of pipes

End condition of pipe or boundary conditions	C - value
Fix - Fix	3.5
Simple - Simple	1.57
Fix-simple	2.45

On the other hand determination of the vortex shedding frequency of free spanning pipe can be obtained by the help of dimensionless term, S_t (Strouhal number), flow velocity and diameter of the pipe;

$$f_{VIV} = \frac{S_t \times V}{D} \tag{2.28}$$

Strouhal number for cylindrical shapes is generally equivalent to 0.2 whenever the Reynolds Number is in between 10^1 to 10^5. Figure 2.6 is showing the relationship between the Reynolds Number and the Strouhal Number for circular cylinders. It is evident that whenever the flow in the system can be defined as

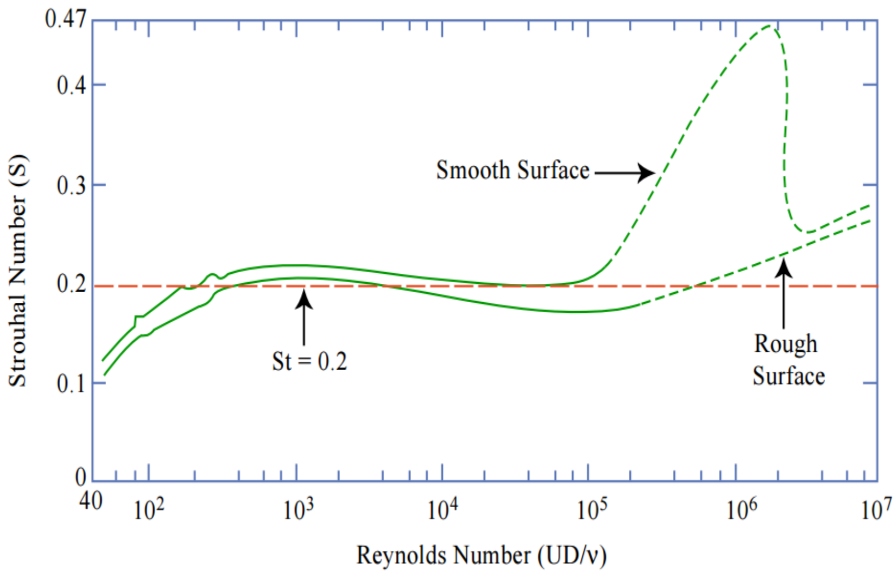

Figure 2.6: Relationship between Strouhal and Reynolds numbers for circular cylinders [29].

2.4.2 Cross- flow Vortex Shedding

The periodic application of forces, as in oscillatory flow conditions, generates vibrations of cylindrical structures mainly because of vortex induced vibrations. These vibrations can be classified into two separate effects which can be resolved as cross flow and inline vibrations. As it was mentioned before, the main reason of cross-flow vibrations is lift force whilst the in-line one is due the potential of drag forces. Both of these vibrations are called vortex induced vibrations. In Excitation in the cross-flow direction is potentially more dangerous than that in the in-line direction since amplitudes of response are much greater than those associated with in-line motion. Cross-flow hydrodynamics the vortex shedding occurrence is related with the reduced velocity which is written as

$$Vr = \frac{u}{f_n D} \tag{2.29}$$

Where u is flow velocity normal to pipe axis, D outer diameter of the pipe and f_n is the natural frequency in water.

Referring to DNV 1981[4] for evaluation of the vortex shedding in cross flow, Figure (2.7) can be used in which Re is represented in x axis and Vr in y axis. The Reynolds number can be calculated by flowing equation:

$$\mathrm{Re} = \frac{u \times D}{\upsilon} \tag{2.30}$$

in which υ is the kinematic viscosity of the sea water which has a magnitude of 1.14×10^{-6} (m^2/s).

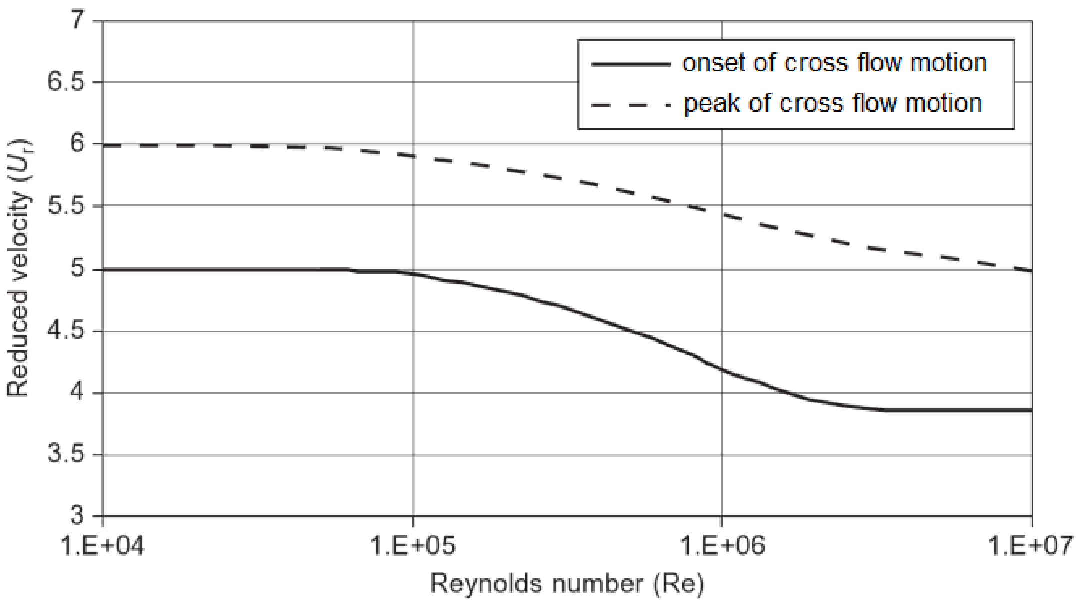

Figure 2.7: Reduced velocity for cross flow oscillations based on the Reynolds number [4].

2.5 Free Spanning Pipelines.

Nowadays there are more challenging for transforming fluid especially water by submerged pipelines due to the increasing demand for rapid transportation facilities throughout the world. Most of the pipeline systems are applied from a start-of point to the end point for instance onshore or other platforms. During the operation of these pipelines changes in seabed topology such as scouring or sand wave, natural hazards like earthquakes or sudden unevenness on formations will result in free span on pipeline transmission systems. As long as the length of the free span is more than the allowable free span of the pipe, consequently the pipeline suffers the fatigue damages on the pipe due to the waves and currents.

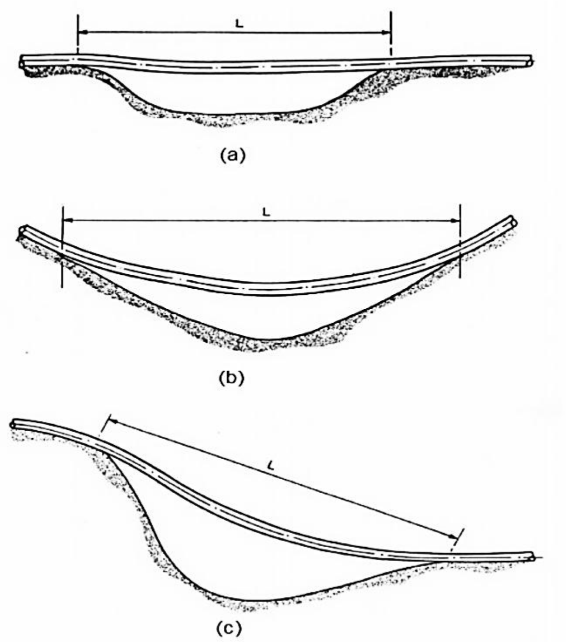

Figure 2.8: Examples of different free span pipeline by Kenny (1993); (a) represents the schematic figure of pipeline crosses seabed depression, (b) is the schematic figure for pipeline crosses for the cases of change in slope and (c) shows the cases where pipeline.

Due to the fluid structure interaction in free spanning regions of spanning pipes oscillations occur due to the hydrodynamic forces. These oscillations may force the pipe to fail as long as the stresses on the pipe become greater than yield stress. As the vortex shedding frequency is synchronized with the natural frequency of the spanning pipe, then resonance creates vibrations on the pipe. This can be prevented if the vortex shedding frequency is sufficiently far from the natural frequency of the pipe span [5].

2.6 Polyethylene pipe (PE)

Polyethylene pipe become very famous due to practical benefits in recent years. Since the early 1950's PE pipes have developments in the production and are increasingly used for various applications. Some of these applications are irrigation systems, drinking water transportation systems, natural gas transmission systems, sewerage and drainage systems, marine condition such that effluent, river and lake crossings, and fresh and salt-water intakes. The major reason for selecting PE pipe and cased to become well-suited for marine conditions is immunity to galvanic corrosion. The combination of air and water, but mainly seawater, can be very corrosive to general metallic piping materials such that steel pipe, [21].

2.6.1 Advantage of PE pipe

PE pipes are very environmentally friendly pipe material and the most application of PE pipes are for potable water transportations especially in marine applications. However the other beneficial features which make PE piping particularly famous for marine applications is [21]:

1- PE pipes are quit light in comparison with other materials and have less density. The weight of PE pipe is approximately one half of cast iron and is less than one tenth of concrete pipe.

2- Due to the fact that PE's density is less than 96% fresh water density and 94% sea water density, the PE pipe can easily stay floating in the water.

3- The PE pipes are made of very flexible materials; therefore, their installations process under the water could be much simpler than other kind of pipelines. Because they could easily adapted in different topographies and they don't need sophisticated equipment for installation and connection. Moreover, because of high flexibility capacity of such pipelines, they will not need extra supporting facilities.

4- Due to its high strain capacity, the PE piping can easily modify to different external forces made by wave and currents. High strain ability also allows the PE piping to safely move or bend to adopt it to altered bedding that can result by the underscoring that may sometimes occur with strong wave and current actions.

2.6.2 Disadvantage of PE pipe

1- Due to their non-decomposing property, plastic pipes are not installed in high temperature.

2- Have rapid crack propagation therefore easily cracked.

3- At higher temperatures, the strength of plastic pipes reduces

4- High coefficient of expansion approximately 0.2

5- Have less resistance against fire.

2.6.3 Height Density Polyethylene (HDPE)

There are a lot of factories produce the PE pipe with different thermal conductivity, mechanical properties, sizes and density generally changes due to basic requests of customer. Among them HDPE pipes and fittings are rapidly becoming the material of select among engineers, contractors and customers for several industry applications, especially in marine operations by use "float-and-sink" method. Around thirty years later, a high-density was created by an American chemist at E.I. by subjecting ethylene to a large amount of pressure. HDPE pipes with high strength-to-density ratio ($0.941 < \text{density} < 0.965$) are thermoplastic material and its main ingredients are carbon and hydrogen atoms and these atoms make high molecular weight. The HDPE pipe is strong, durable, flexible and light weight, has good barrier properties, fatigue resistant and stiffness. In comparison with other plastic materials HDPE became more suitable for marine structure. The comparison of different material properties is given in Table 2.4 [22] and the physical material properties of HDPE pipes are given in Table 2.5.

Table 2.3: Comparison HDPE with other plastic materials [22]

Property	HDPE	PP	PVC	PVC-C*	PB*
Surface feel	Waxy	Waxy	Smooth	Smooth	Waxy
Appearance (water pipes)	Black	Pale grey-beige	Blue	Grey-beige	Black
Sound produced when dropped	Medium clatter	High clatter	High clatter	High clatter	Dull thud
Combustibility and appearance of	Drops continue to burn after falling	Drops continue to burn after falling	Carbonizes Extinguishes away	Carbonizes Extinguishes away	Drops continue to burn after falling
Odour of smoke extinguished	Like candles	Like resin	Pungent like hydrochloric acid	Pungent like hydrochloric acid	Like candles but more acrid than HDPE
Nail test (impression made	Impression possible	Very light impression possible	Impression not possible	Impression not possible	Impression easily produced
Special features	-----	-----	------	-----	Smears when sawn
Floats in water	Yes	Yes	No	No	Yes
Notch sensitivity	No	Slight	Yes	Yes	Yes
Weather resistance	Stabilized, good	Stabilized, good	Stabilized, good	Stabilized, good	Stabilized, good
Method of permanent joining	Fusion	Fusion	Solvent cement	Solvent cement	Fusion
Suitable for mechanical jointing	Yes	Yes	Yes	Yes	Yes
Stress crack sensitivity with regard to jointing with save media, e.g water	Some	Slight	None	None	None
Linear expansion mm/m/ºC	0.2	0.15	0.08	0.07	0.12
Thermal conductivity kcal/ mhºC	0.4	0.19	0.14	0.14	0.2
Passion ratio mhºC	0.42	0.4	0.23	0.23	0.47
Density kg/cm²	0.960	0.905	1.42	1.5	0.92
Tensile strength at 20ºC kp/cm²	240	320	550	550	200
Modulus of elasticity at 20ºC kp/cm²	12000	15000	30000	30000	5000

HDPE : high density polyethylene pipe

PP : polypropylene pipe

PVC : polyvinyl chloride pipe

PVC-C : Chlorinated Polyvinyl Chloride

PB : polybutylene pipe

Table 2.4: Material properties of HDPE pipes.

Property	Standard	Unit	PE 80	PE 100	PP-R
Density	DIN 53479 ISO 178	g/cm3	0.95	0.96	0.91
tensile modulus	ISO 178	N/mm2	170	1200	160
yield stress	DIN 53495	N/mm2	23	25	26
tensile strength	DIN 53495	N/mm2	32	38	15
Elongation at break	DIN 53495	%	>600	>600	>50
ball indentation hardness	ISO 178	N/mm2	42	46	45
coefficient of linear thermal expansion	DIN 53752	1/ºC	1.8 x 10-4	1.8 x 10-4	1.6 x 10-4

2.7 Summary of the Chapter

In this Chapter all the hydrodynamic variables that are effective on calculating the velocity around the circular pipes, forces acting on horizontal and vertical directions and material properties of HDPE pipes are analyzed and discussed. All the constant parameters which are effective on calculating wave forces and vortexes around pipes are discussed. Next chapter will deal with the calculations of orbital velocities, current velocities and the net velocities around spanning circular pipes. All the calculations will be performed based on the MATLAB code developed for this study.

Chapter 3

Cross-line and Inline Force Modeling

3.1 Overview

In this chapter all the principal information about the investigated pipe model and the flow current simulation will be described in detail. Polyethylene pipes with different diameters and different lengths are going to be modeled regarding the DIN8074 [10] guidelines for such pipelines. This standard demonstrates dimensions for pipes made of polyethylene (PE). It is directed at manufacturers and users of PE pressure pipes. It is projected to afford the user with a fundamental description which includes the dimensions for pressure pipes made of polyethylene (PE). In general, the standard covers features of quality. By this standard DIN 8074 [10], the public is simultaneously provided with the revised standard DIN 8075[25], which specifies the general quality requirements and tests for these pipes.

The finite element ANSYS software [27] is allocated for 3D analysis for the pipes and the internal flow current modeling. To accomplish this procedure, the Static Structural Analysis using Mechanical APDL Solver part will be used to investigate the pipeline's structural behavior under sea current and pressure. To assess the external flow around pipeline and evaluation all the necessary parameters with their effects to pipeline, the MATLAB software is used.

3.2 Environmental parameters of the problem.

The DNV-RP-C205 [8] and DNV-OS-F101 [1] are the general codes that are accepted all around the world. Here, in this study these codes will be used as guiding documents for this study. The environmental limitations of this study starts with the intermediate depth assumptions in which wave height can be effective to generate momentum forces but not enough orbital velocity to generate vortex induced vibration at the sea bottom. Therefore, the limits on Keulegan-Carpenter as between 4 and 7 will be maintained. Also, in this research, subcritical flow conditions must be pervading around the pipe such that pair of vortex can be observed around the pipe. This can only be achieved when flow Reynolds Number is below or around 3.5×10^{5}. In the case of current velocity occurrences at the bottom of the sea, the effect of current velocity is also added to the physical environment of the research study. In order to be able to calculate the current velocity, it was important to define the sea depth where submerged pipes were located. The initial assumption that the spanning length of the pipes will occur at intermediate depths ($\lambda/20 < d < \lambda/2$) was successfully used while deciding the magnitude of current velocity. The resultant depths were 26 to 30 meters in the sea.

In order to initiate the analyses the wave data that will fit the above mentioned criteria and assumptions were used as an input variable to the analysis. These input variables were the wave height, H, wave period, T, and the depth of the sea, d, in which spanning of the submerged pipes are assumed to occur. Evidently to be able to minimize the level and percentage of mistakes during the research, a comparative process based on different information resources is practical. In order to achieve this, the analyses are carried out MATLAB software, which is given in Appendix A.

3.2.1 The net velocity around the spanning pipeline

Starting with the assumptions of intermediate wave conditions, the wave height at deep water should be transferred by the help of shoaling coefficient to the new wave height.

$$H_{new} = K_s \times H_o \tag{3.1}$$

In which K_s represents the shoaling coefficient, H_o is the deep water wave height and H_{new} is the wave height at intermediate depth zone. The shoaling coefficient can be directly read from “Gravity Wave Table” or can be calculated by the help of the ratio between the group wave celerity [16].

$$K_s = \sqrt{\frac{C_o n_o}{C_1 n_1}} \tag{3.2}$$

In which C_o is the wave celerity at deep water depth and n_o is equivalent to 0.5 at deep water. C_1 is the wave celerity at intermediate depth and n_1 can be calculated as

$$n_1 = \frac{1}{2}[1 + \frac{(4\pi d / \lambda)}{\sinh(4\pi d / \lambda)}] \tag{3.3}$$

The orbital velocity of waves, the current velocity and the net velocity of flow around the pipe is therefore calculated by the help of MATLAB code which is developed for this thesis. The results for different wave heights and depths and for constant wave period are given in Tables (3.1), (3.2) and (3.3). In all tables the highlighted parts show that calculated values are out of limitations.

Table 3.1: The orbital, current and total velocities around the pipe with diameter, D=0.8 m

H (m)	**T (sec)**	**e/D**	**λ (m)**	**λ_{new} (m)**	**K_S**	**H_{new} (m)**	**U_C (m/s)**	**U_X (m/s)**	**U_T (m/s)**
d= 26 (m)									
2.3	8	0.1	99.84	96.3	0.93	2.1	0.17	0.31	0.48
2.5	8	0.1	99.84	96.3	0.93	2.3	0.19	0.33	0.52
2.8	8	0.1	99.84	96.3	0.93	2.6	0.21	0.38	0.59
3	8	0.1	99.84	96.3	0.93	2.8	0.22	0.41	0.63
d= 27 (m)									
2.3	8	0.1	99.84	96.3	0.94	2.2	0.16	0.29	0.45
2.5	8	0.1	99.84	96.3	0.94	2.3	0.17	0.32	0.49
2.8	8	0.1	99.84	96.3	0.94	2.6	0.2	0.35	0.55
3	8	0.1	99.84	96.3	0.94	2.8	0.21	0.38	0.59
d = 28 (m)									
2.3	8	0.1	99.84	96.3	0.95	2.2	0.15	0.28	0.43
2.5	8	0.1	99.84	96.3	0.95	2.4	0.16	0.31	0.47
2.8	8	0.1	99.84	96.3	0.95	2.6	0.18	0.34	0.52
3	8	0.1	99.84	96.3	0.95	2.9	0.2	0.36	0.56
d = 29 (m)									
2.3	8	0.1	99.84	96.67	0.95	2.2	0.14	0.26	0.4
2.5	8	0.1	99.84	96.67	0.95	2.4	0.15	0.29	0.44
2.8	8	0.1	99.84	96.67	0.95	2.6	0.17	0.31	0.49
3	8	0.1	99.84	96.67	0.95	2.8	0.19	0.34	0.53
d = 30 (m)									
2.3	8	0.1	99.84	96.77	0.96	2.2	0.13	0.25	0.38
2.5	8	0.1	99.84	96.77	0.96	2.4	0.14	0.27	0.41
2.8	8	0.1	99.84	96.77	0.96	2.7	0.16	3	0.46
3	8	0.1	99.84	96.77	0.96	2.8	0.17	0.33	0.5

Column 4 is calculated by Equation 2.2, Column 5 is calculated by check with intermediate depth, Column 6 is calculated by Equation 3.2, Column 7 is calculated by Equation 3.1, Column 8 is calculated by Equation 2.8 and Column 9 is calculated by Equation 2.6, column 10 is added by column 5 and 6.

Table 3.2: The orbital, current and total velocities around the pipe with diameter, D=0.7 m

H (m)	T (sec)	e/D	ʎ (m)	$ʎ_{new}$ (m)	K_S	H_{new} (m)	U_C (m/s)	U_X (m/s)	U_T (m/s)
d= 26 (m)									
2.3	8	0.1	99.84	96.3	0.93	2.1	0.16	0.31	0.47
2.5	8	0.1	99.84	96.3	0.93	2.3	0.18	0.34	0.52
2.8	8	0.1	99.84	96.3	0.93	2.6	0.2	0.38	0.58
3	8	0.1	99.84	96.3	0.93	2.8	0.22	0.41	0.63
d= 27 (m)									
2.3	8	0.1	99.84	96.43	0.94	2.15	0.16	0.29	0.45
2.5	8	0.1	99.84	96.43	0.94	2.34	0.17	0.32	0.49
2.8	8	0.1	99.84	96.43	0.94	2.62	0.19	0.36	0.55
3	8	0.1	99.84	96.43	0.94	2.81	0.21	0.38	0.59
d = 28 (m)									
2.3	8	0.1	99.84	96.3	0.95	2.2	0.15	0.28	0.43
2.5	8	0.1	99.84	96.3	0.95	2.4	0.16	0.31	0.47
2.8	8	0.1	99.84	96.3	0.95	2.6	0.18	0.34	0.52
3	8	0.1	99.84	96.3	0.95	2.9	0.2	0.35	0.55
d = 29 (m)									
2.3	8	0.1	99.84	96.67	0.95	2.2	0.14	0.26	0.4
2.5	8	0.1	99.84	96.67	0.95	2.4	0.15	0.29	0.44
2.8	8	0.1	99.84	96.67	0.95	2.6	0.17	0.31	0.49
3	8	0.1	99.84	96.67	0.95	2.8	0.19	0.34	0.53
d = 30 (m)									
2.3	8	0.1	99.84	96.77	0.96	2.2	0.13	0.25	0.38
2.5	8	0.1	99.84	96.77	0.96	2.4	0.14	0.27	0.41
2.8	8	0.1	99.84	96.77	0.96	2.7	0.16	3	0.46
3	8	0.1	99.84	96.77	0.96	2.8	0.17	0.33	0.5

Column 4 is calculated by Equation 2.2, Column 5 is calculated by check with intermediate depth, Column 6 is calculated by Equation 3.2, Column 7 is calculated by Equation 3.1, Column 8 is calculated by Equation 2.8 and Column 9 is calculated by Equation 2.6, column 10 is added by column 5 and 6.

Table 3.3: The orbital, current and total velocities around the pipe with diameter, D=0.6 m

H (m)	**T (sec)**	**e/D**	**λ (m)**	**λ_{new} (m)**	**K_S**	**H_{new} (m)**	**U_C (m/s)**	**U_X (m/s)**	**U_T (m/s)**
d= 26 (m)									
2.3	8	0.1	99.84	96.43	0.94	2.14	0.16	0.31	0.47
2.5	8	0.1	99.84	96.43	0.94	2.33	0.18	0.34	0.52
2.8	8	0.1	99.84	96.43	0.94	2.61	0.2	0.37	0.57
3	8	0.1	99.84	96.43	0.94	2.8	0.21	0.41	0.62
d= 27 (m)									
2.3	8	0.1	99.84	96.43	0.94	2.15	0.15	0.3	0.45
2.5	8	0.1	99.84	96.43	0.94	2.34	0.17	0.32	0.49
2.8	8	0.1	99.84	96.43	0.94	2.62	0.19	0.35	0.54
3	8	0.1	99.84	96.43	0.94	2.81	0.2	0.38	0.58
d = 28 (m)									
2.3	8	0.1	99.84	96.55	0.95	2.16	0.14	0.28	0.42
2.5	8	0.1	99.84	96.55	0.95	2.35	0.16	0.30	0.46
2.8	8	0.1	99.84	96.55	0.95	2.63	0.18	0.33	0.51
3	8	0.1	99.84	96.55	0.95	2.82	0.19	0.36	0.55
d = 29 (m)									
2.3	8	0.1	99.84	96.67	0.95	2.18	0.14	0.26	0.4
2.5	8	0.1	99.84	96.67	0.95	2.36	0.15	0.28	0.43
2.8	8	0.1	99.84	96.67	0.95	2.64	0.17	0.31	0.48
3	8	0.1	99.84	96.67	0.95	2.83	0.18	0.34	0.52
d = 30 (m)									
2.3	8	0.1	99.84	96.77	0.96	2.18	0.13	0.24	0.37
2.5	8	0.1	99.84	96.77	0.96	2.37	0.14	0.27	0.41
2.8	8	0.1	99.84	96.77	0.96	2.65	0.16	3	0.46
3	8	0.1	99.84	96.77	0.96	2.84	0.17	0.32	0.49

Column 4 is calculated by Equation 2.2, Column 5 is calculated by check with intermediate depth, Column 6 is calculated by Equation 3.2, Column 7 is calculated by Equation 3.1, Column 8 is calculated by Equation 2.8 and Column 9 is calculated by Equation 2.6, column 10 is added by column 5 and 6.

3.2.2 Analysis of forces around the spanning pipe

Although the vortex induced vibration is the main concern for most of the research studies, a pair of vortex can even be critical for the failure of the pipes. Figure 3.1 shows the relationship between Keulegan-Carpenter number and the Reynolds number. As can be observed from Figure 3.1 the effects of vortex shedding occurs when Keulegan-Carpenter number is greater than 7. Therefore, here in this study cross-line and in- line forces will be evaluated when only a pair of vortex is active around the submerged pipes.

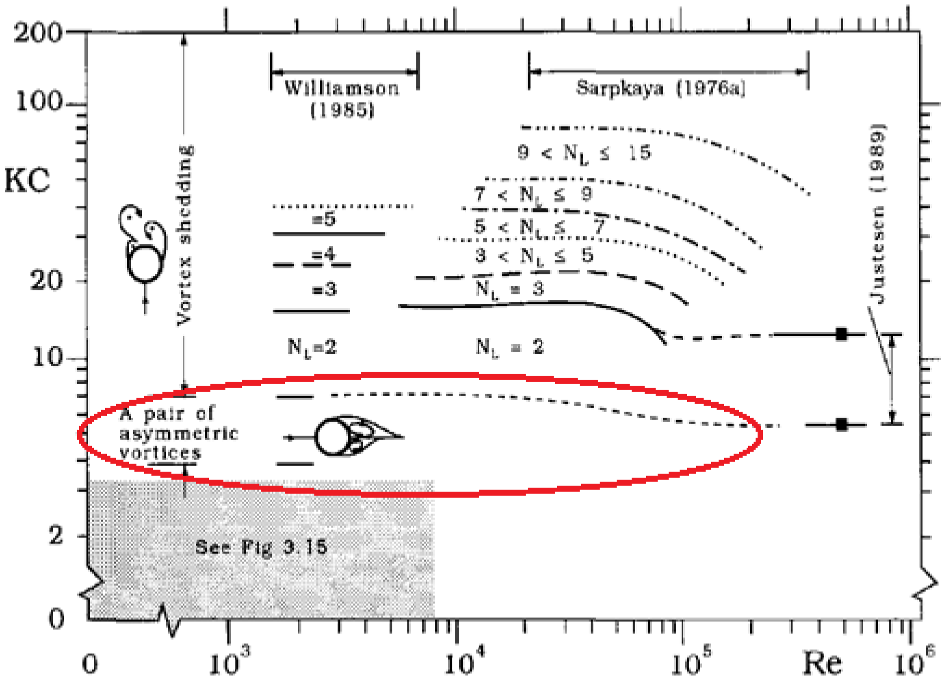

Figure 3.1: Vortex shedding regimes around a smooth circular cylinder [5]

3.2.2.1 In-line wave forces

Based on the definitions given in Chapter 2 and the assumptions considered for this research the in-line forces acting on the spanning pipe are analyzed. In-line forces as described before are represented in combination of drag force, hydrodynamic force and Froude–Krylov force. To precede the calculation process accurately and make the data more trustable, the MATLAB code is used. Some of the results shown in the following tables (Table 3.4, 3.5 and 3.6) are labelled with color. This is because some of the results were not in the limits of $4 < KC < 7$ and Re smaller than 3.5×10^5. These results were not used in the following analyses while calculating the spanning length of submerged pipes. In these tables total in-line forces are determined by adding the magnitude of Inertia force and Froude Krylov number at the same wave period. According to in-line force equation, maximum drag force occur when horizontal velocity is maximum which means that phase angle θ is equivalent to 0 or 2π. In addition maximum horizontal velocity in the negative direction occurs when phase angle θ is equivalent to π or 3π.

Table 3.4: Total inline force on spanning pipe for D= 0.8 m

H (m)	**T** (Sec)	C_D ---	C_I ----	F_{hyd} (N)	F_P (N)	**max** F_D (N)	**KC**	**Re**	**Total Inline forces** (N)
d = 26(m)									
2.3	8	0.7	1.82	189.99	125.37	66.32	4.8	3.4	315.36
2.5	8	0.7	1.76	206.51	136.27	78.36	5.2	3.7	342.78
2.8	8	0.7	1.68	231.29	152.62	98.29	5.8	4.1	383.91
3	8	0.7	1.62	163.53	247.81	112.83	6.27	4.4	411.34
d = 27 (m)									
2.3	8	0.7	1.86	179.58	118.51	59.03	4.5	3.2	298.09
2.5	8	0.7	1.8	128.81	195.2	69.74	4.9	3.5	324.01
2.8	8	0.7	1.72	144.27	218.62	87.49	5.5	3.9	362.89
3	8	0.7	1.66	154.57	234.34	100.43	5.9	4.2	388.91
d= 28 (m)									
2.3	8	0.7	1.9	111.98	169.69	52.51	4.3	3	281.67
2.5	8	0.7	1.84	121.71	184.45	62.04	4.6	3.3	306.16
2.8	8	0.7	1.76	136.32	206.58	77.83	5.2	3.7	342.9
3	8	0.7	1.72	146.06	221.34	89.34	5.6	3.9	367.4
d=29 (m)									
2.3	8	0.7	1.94	105.77	160.29	46.69	4	2.8	266.06
2.5	8	0.7	1.88	114.97	174.22	55.16	4.4	3.1	289.19
2.8	8	0.7	1.82	128.77	195.13	69.19	4.9	3.4	323.9
3	8	0.7	1.76	137.96	209.07	79.43	5.3	3.7	347.03
3.2	8	0.7	1.72	147.16	223.01	90.38	5.6	3.9	370.17
d=30 (m)									
2.3	8	0.7	1.96	99.78	151.35	41.49	3.8	2.7	251.13
2.5	8	0.7	1.92	108.56	164.51	49.01	4.13	2.9	273.07
2.8	8	0.7	1.86	121.58	184.25	61.48	4.6	3.2	305.83
3	8	0.7	1.8	130.27	197.41	70.58	5	3.5	327.68
3.2	8	0.7	1.76	138.95	210.57	80.3	5.3	3.7	349.52

Column 5 is calculated by Equation 2.12, Column 6 is calculated by Equation 2.13

Column 7 is calculated by Equation 2.9, Column 8 is calculated by Equation 2.24

Column 9 is calculated by Equation 2.30 and Column 10 is added by column 5 and 6.

Table 3.5: Total inline force on spanning pipe for D= 0.7 m

H (m)	**T** (Sec)	**C_D** ---	**C_I** ----	**F_{hyd}** (N)	**F_P** (N)	**max F_D** (N)	**KC**	**Re**	**Total Inline forces** (N)
d = 26(m)									
2.3	8	0.7	1.92	95.98	145.45	57.25	5.40	2.90	241.43
2.5	8	0.7	1.86	104.32	158.02	67.63	5.90	3.20	262.42
2.8	8	0.7	1.78	116.84	177.06	84.84	6.80	3.60	293.91
3	8	0.7	1.74	125.15	189.71	97.39	7.10	3.80	314.9
d = 27 (m)									
2.3	8	0.7	1.94	90.72	137.48	50.96	5.10	2.80	228.21
2.5	8	0.7	1.9	98.61	149.44	60.20	5.60	3.00	247.35
2.8	8	0.7	1.82	110.45	167.37	75.52	6.30	3.40	278.72
3	8	0.7	1.78	118.34	179.33	86.69	6.70	3.60	297.66
d= 28 (m)									
2.3	8	0.7	1.98	85.73	129.91	45.33	4.90	2.60	215.64
2.5	8	0.7	1.94	93.18	141.21	53.56	5.30	2.80	234.39
2.8	8	0.7	1.86	104.36	158.15	67.18	5.90	3.20	262.51
3	8	0.7	1.82	111.82	169.45	77.1	6.30	3.40	281.26
3.2	8	0.7	1.78	119.27	180.74	87.75	6.80	3.60	300.01
d=29 (m)									
2.3	8	0.7	2	80.97	122.71	40.31	4.50	2.50	203.68
2.5	8	0.7	1.96	94.31	133.38	47.62	5.00	2.70	221.40
2.8	8	0.7	1.9	105.63	149.39	59.73	5.60	3.00	247.96
3	8	0.7	1.86	105.62	160.06	68.57	6.00	3.20	268.68
3.2	8	0.7	1.82	112.66	170.73	78.02	6.40	3.40	283.39
d=30 (m)									
2.3	8	0.79	2	76.46	115.87	35.81	4.32	2.30	192.33
2.5	8	0.7	2	83.11	125.94	42.31	4.70	2.50	209.05
2.8	8	0.7	1.94	93.08	141.05	53.08	5.30	2.80	234.14
3	8	0.7	1.9	99.73	151.13	60.93	5.60	3.00	250.86
3.2	8	0.7	1.86	106.37	161.21	69.33	6.00	3.20	267.58

Column 5 is calculated by Equation 2.12, Column 6 is calculated by Equation 2.13

Column 7 is calculated by Equation 2.9, Column 8 is calculated by Equation 2.24

Column 9 is calculated by Equation 2.30 and Column 10 is added by column 5 and 6.

Table 3.6: Total inline force on spanning pipe for D= 0.6 m

H (m)	T (Sec)	C_D ---	C_I ----	F_{hyd} (N)	F_P (N)	max F_D (N)	KC	Re	Total Inline forces (N)
d = 26(m)									
2.3	8	0.7	2	70.51	106.85	48.31	6.3	2.5	177.36
2.5	8	0.7	1.96	76.64	116.14	57.08	6.9	2.7	192.78
2.8	8	0.7	1.9	85.84	130.08	71.60	7.7	3	215.92
3	8	0.7	1.8	91.97	139.37	82.2	8.2	3.3	231.34
d = 27 (m)									
2.3	8	0.7	2	66.65	101	43.01	5.9	2.4	167.65
2.5	8	0.7	1.98	72.45	109.78	50.81	6.5	2.6	182.23
2.8	8	0.7	1.92	81.14	122.96	63.74	7.7	2.9	204.10
3	8	0.7	1.88	86.93	131.74	73.17	7.8	3.1	218.67
d= 28 (m)									
2.3	8	0.8	2	62.98	95.44	38.26	5.6	2.2	158.42
2.5	8	0.7	2	68.45	103.74	45.21	6.1	2.4	172.19
2.8	8	0.7	1.98	76.67	116.18	56.71	6.8	2.6	192.85
3	8	0.7	1.92	146.06	221.34	89.34	7.3	2.9	367.4
d=29 (m)									
2.3	8	0.83	2	59.49	90.15	34.02	5.3	2.1	149.64
2.5	8	0.79	2	64.66	97.99	40.20	5.8	2.3	162.65
2.8	8	0.7	2	72.42	109.75	50.02	6.5	2.5	182.17
3	8	0.7	1.96	137.96	209.07	79.43	6.9	2.7	347.03
d=30 (m)									
2.3	8	0.86	2	56.17	85.12	30.23	5	2	141.29
2.5	8	0.83	2	61.05	92.52	35.72	5.4	2.1	153.58
2.8	8	0.7	2	68..38	103.63	44.81	6	2.4	172.01
3	8	0.7	1.98	73.27	111.03	51.44	6.5	2.6	184.29

Column 5 is calculated by Equation 2.12, Column 6 is calculated by Equation 2.13

Column 7 is calculated by Equation 2.9, Column 8 is calculated by Equation 2.24

Column 9 is calculated by Equation 2.30 and Column 10 is added by column 5 and 6.

The calculation of in-line and cross-flow forces has shown that the e/D ratio is important to understand the limitation for different lift force in cross-flow vibration. By the help of generated MATLAB code several different e/D ratios are used to definite the ratio between in-line forces and Cross-flow forces.

It is observed that when e/D > 1 the important of lift force vanishes compared to the in-line forces. This means that important of the cross flow vibration becomes negligible and in-line vibrations dominate behavior of the pipe as shown inFigure 3.2.

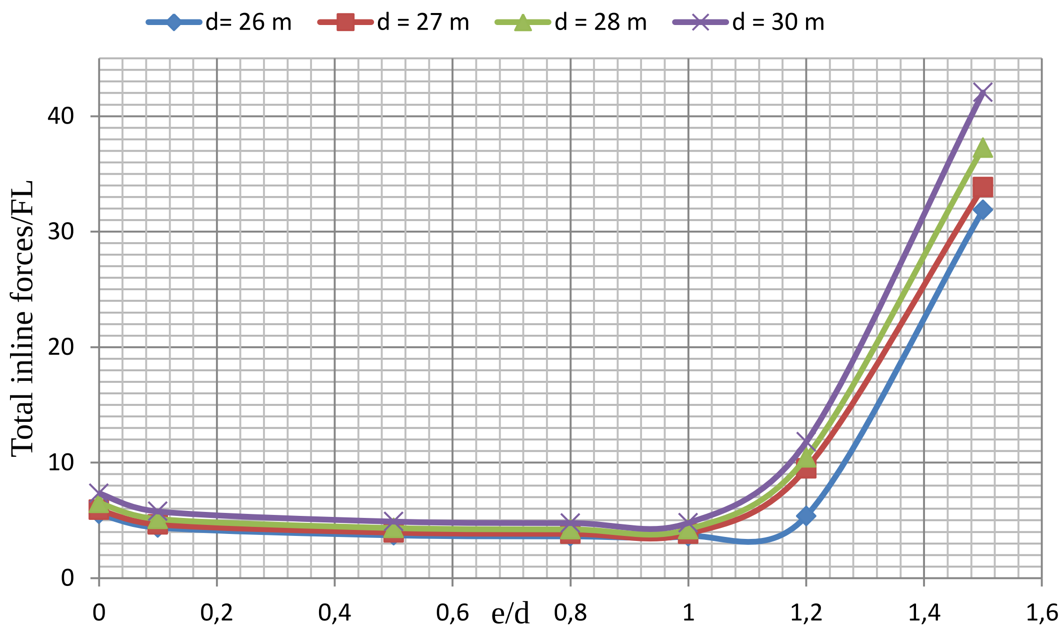

Figure 3.2: The steep change in ratio of total In-line forces to lift force when e/D becomes quarter than 1 for different depths.

3.2.2.2 Cross wave forces

Since the orbital wave velocity of decreases as one goes deeper, the magnitude of inline forces was not effective in the stability of spanning pipes. On the other hand, the cross line forces like weight of the pipe and fluid inside it becomes important when the vertical forces are concerned. Cross wave forces are including lift force, buoyant force and total mass of the pipe. The total mass can be considered as addition of pipe mass, pipe content and added mass. Added mass is accepted to represent the inertia added to a system because of accelerating or decelerating of moving body submerged in the fluid. For simplicity it is usually modeled as volume of fluid moving with the object. The total mass is therefore, can be given in terms of weight by the following equations:

$$W_P = \rho_{pipe} g \frac{\pi}{4}\left(D_0^2 - D_I^2\right) \tag{3.3}$$

$$W_C = \rho_{flow} g \frac{\pi}{4}\left(D_I^2\right) \tag{3.4}$$

$$W_A = \rho_{fluid} g C_a \frac{\pi}{4}\left(D_0^2\right) \tag{3.5}$$

In which W_p represents the weight of the pipe, W_c represents the weight of the fluid flowing in the pipe and W_A represents the weight of added mass. D_0 and D_I are the outer and inner diameters of the pipe. The dimensionless added mass coefficient is the ratio between the added mass and the displaced fluid mass. For circular cylinders the added mass coefficient is taken as 1. As has been shown in Figure 2.1 the total cross force is determined by the subtraction of total mass from lift force and buoyancy force. All these calculations are followed by the help of MATLAB code which has been given in APPENDIX A. Since the density of water is greater than the density of HDPE pipes the minimum thickness values of HDPE pipes are used in order to estimate maximum possible cross line forces. The thicknesses and pipe diameters are chosen from DIN 8074 [10] in which D=0.8 m, D=0.7m, D=0.6m were considered. The resultant cross line forces can be read from Tables 3.7, 3.8, 3.9. Some of the results shown in the following tables (Table 3.7, 3.8 and 3.9) are labelled with color. This is because some of the results were not in the limits of $4 < KC < 7$ and Re smaller than 3.5×10^5. These results were not used in the following analyses while calculating the spanning length of submerged pipes.

Table 3.7: Total cross-flow forces for D=0.8 m

H (m)	T (sec)	C_L -----	F_L (N)	F_B (N)	W of pipe (N)	W of content (N)	W of added mass (N)	kc	Re $\times 10^5$	Total cross Force (N)
d = 26 (m)										
2.3	8	0.7	66.32	5046.8	364.1	4549.2	5046.8	4.8	3.4	4847.1
2.5	8	0.7	78.36	5046.8	364.1	4549.2	5046.8	5.2	3.7	4835.1
2.8	8	0.7	98.29	5046.8	364.1	4549.2	5046.8	5.8	4.1	4815.1
3	8	0.7	112.8	5046.8	364.1	4549.2	5046.8	6.27	4.4	4800.5
d = 27 (m)										
2.3	8	0.7	59.03	5046.8	364.1	4549.2	5046.8	4.5	3.2	4854.3
2.5	8	0.7	69.74	5046.8	364.1	4549.2	5046.8	4.9	3.5	4843.6
2.8	8	0.7	87.49	5046.8	364.1	4549.2	5046.8	5.5	3.9	4825.9
3	8	0.7	100.4	5046.8	364.1	4549.2	5046.8	5.9	4.2	4812.9
d= 28(m)										
2.3	8	0.7	52.51	5046.8	364.1	4549.2	5046.8	4.3	3	4860.9
2.5	8	0.7	62.04	5046.8	364.1	4549.2	5046.8	4.6	3.3	4851.3
2.8	8	0.7	77.83	5046.8	364.1	4549.2	5046.8	5.2	3.7	4835.5
3	8	0.7	89.34	5046.8	364.1	4549.2	5046.8	5.6	3.9	4824.0
d=29(m)										
2.3	8	0.7	46.69	5046.8	364.1	4549.2	5046.8	4	2.8	4866.7
2.5	8	0.7	55.16	5046.8	364.1	4549.2	5046.8	4.4	3.1	4858.2
2.8	8	0.7	69.19	5046.8	364.1	4549.2	5046.8	4.9	3.4	4844.2
3	8	0.7	79.43	5046.8	364.1	4549.2	5046.8	5.3	3.7	4833.9
3.2	8	0.7	90.38	5046.8	364.1	4549.2	5046.8	5.6	3.9	4823.0
d=30(m)										
2.3	8	0.7	41.49	5046.8	364.1	4549.2	5046.8	3.8	2.7	4871.9
2.5	8	0.7	49.01	5046.8	364.1	4549.2	5046.8	4.13	2.9	4864.4
2.8	8	0.7	61.48	5046.8	364.1	4549.2	5046.8	4.6	3.2	4851.9
3	8	0.7	70.58	5046.8	364.1	4549.2	5046.8	5	3.5	4842.8
3.2	8	0.7	80.3	5046.8	364.1	4549.2	5046.8	5.3	3.7	4833.1

Column 4 is calculated by Equation 2.23, Column 5 is calculated by Equation 2.21 Column 6 is calculated by Equation 3.3, Column 7 is calculated by Equation 3.4, Column 8 is calculated by Equation 3.5, Column 9 is calculated by 2.24, column 10 is calculated by 2.30, and column 11 is subtraction of column 6, 7 and 8 by column 4 and 5.

Table 3.8: Total cross-flow forces for D=0.7 m.

H (m)	T (sec)	C_L -----	F_L (N)	F_B (N)	W of pipe (N)	W of content (N)	Wof added mass (N)	kc	Re $\times 10^5$	Total cross Force (N)
2.3	8	0.7	57.3	3863.98	276.05	3479.6	3863.96	5.40	2.90	3685.1
2.5	8	0.7	67.6	3863.98	276.05	3479.6	3863.96	5.90	3.20	3674.7
2.8	8	0.7	84.8	3863.98	276.05	3479.6	3863.96	6.80	3.60	3657.5
3	8	0.7	97.4	3863.98	276.05	3479.6	3863.96	7.10	3.80	3644.9
d = 27 (m)										
2.3	8	0.7	51.0	3863.98	276.05	3479.6	3863.96	5.10	2.80	3691.3
2.5	8	0.7	60.2	3863.98	276.05	3479.6	3863.96	5.60	3.00	3682.1
2.8	8	0.7	75.5	3863.98	276.05	3479.6	3863.96	6.30	3.40	3666.8
3	8	0.7	86.7	3863.98	276.05	3479.6	3863.96	6.70	3.60	3655.6
d= 28(m)										
2.3	8	0.7	45.3	3863.98	276.05	3479.6	3863.96	4.90	2.60	3697.0
2.5	8	0.7	53.6	3863.98	276.05	3479.6	3863.96	5.30	2.80	3688.7
2.8	8	0.7	67.2	3863.98	276.05	3479.6	3863.96	5.90	3.20	3675.1
3	8	0.7	77.1	3863.98	276.05	3479.6	3863.96	6.30	3.40	3665.2
3.2	8	0.7	87.8	3863.98	276.05	3479.6	3863.96	6.80	3.60	3654.6
d=29(m)										
2.3	8	0.7	40.3	3863.98	276.05	3479.6	3863.96	4.50	2.50	3702.0
2.5	8	0.7	47.6	3863.98	276.05	3479.6	3863.96	5.00	2.70	3694.7
2.8	8	0.7	59.7	3863.98	276.05	3479.6	3863.96	5.60	3.00	3682.6
3	8	0.7	68.6	3863.98	276.05	3479.6	3863.96	6.00	3.20	3673.7
3.2	8	0.7	78.0	3863.98	276.05	3479.6	3863.96	6.40	3.40	3683.91
d=30(m)										
2.3	8	0.74	35.8	3863.98	276.05	3479.6	3863.96	4.32	2.30	3706.5
2.5	8	0.7	42.3	3863.98	276.05	3479.6	3863.96	4.70	2.50	3700.0
2.8	8	0.7	53.1	3863.98	276.05	3479.6	3863.96	5.30	2.80	3689.2
3	8	0.7	60.9	3863.98	276.05	3479.6	3863.96	5.60	3.00	3681.4
3.2	8	0.7	69.3	3863.98	276.05	3479.6	3863.96	6.00	3.20	3673.0

Column 4 is calculated by Equation 2.23, Column 5 is calculated by Equation 2.21 Column 6 is calculated by Equation 3.3, Column 7 is calculated by Equation 3.4, Column 8 is calculated by Equation 3.5, Column 9 is calculated by 2.24, column 10 is calculated by 2.30, and column 11 is subtraction of column 6, 7 and 8 by column 4 and 5.

Table 3.9: Total cross-flow forces for D=0.6 m.

H (m)	**T** (sec)	**C_L** ---	**F_L** (N)	**F_B** (N)	**W of pipe** (N)	**W of content** (N)	**W of added mass** (N)	**KC**	**Re** $\times 10^5$	**Total cross Force** (N)
d=26 (m)										
2.3	8	0.7	48.31	2838.8	213.8	2549.6	2838.8	6.3	2.5	2715.0
2.5	8	0.7	57.08	2838.8	213.8	2549.6	2838.8	6.9	2.7	2706.3
2.8	8	0.7	71.6	2838.8	213.8	2549.6	2838.8	7.7	3	2691.8
3	8	0.7	82.2	2838.8	213.8	2549.6	2838.8	8.2	3.3	2681.8
d = 27(m)										
2.3	8	0.72	43.1	2838.8	213.8	2549.6	2838.8	5.9	2.4	2720.3
2.5	8	0.7	50.81	2838.8	213.8	2549.6	2838.8	6.5	2.6	2712.5
2.8	8	0.7	63.74	2838.8	213.8	2549.6	2838.8	7.7	2.9	2699.6
3	8	0.7	73.17	2838.8	213.8	2549.6	2838.8	7.8	3.1	2690.2
d= 28(m)										
2.3	8	0.76	38.26	2838.8	213.8	2549.6	2838.8	5.6	2.2	2725.1
2.5	8	0.72	45.21	2838.8	213.8	2549.6	2838.8	6.1	2.4	2718.1
2.8	8	0.7	56.71	2838.8	213.8	2549.6	2838.8	6.8	2.7	2706.6
3	8	0.7	65.1	2838.8	213.8	2549.6	2838.8	7.3	2.9	2698.3
3.2	8	0.7	74.07	2838.8	282.0	3479.6	2838.8	7.8	3.1	2757.6
d=29(m)										
2.3	8	0.78	34.02	2838.8	213.8	2549.6	2838.8	5.3	2.1	2729.3
2.5	8	0.74	40.2	2838.8	213.8	2549.6	2838.8	5.8	2.3	2723.2
2.8	8	0.7	50.42	2838.8	213.8	2549.6	2838.8	6.5	2.5	2713.3
3	8	0.7	57.88	2838.8	213.8	2549.6	2838.8	6.9	2.7	2705.5
3.2	8	0.7	65.86	2838.8	213.8	2549.6	2838.8	7.4	2.9	2697.5
d=30(m)										
2.3	8	0.8	30.23	2838.8	213.8	2549.6	2838.8	5	2	2733.1
2.5	8	0.78	35.72	2838.8	213.8	2549.6	2838.8	5.4	2.1	2727.6
2.8	8	0.72	44.81	2838.8	213.8	2549.6	2838.8	6	2.4	2718.5
3	8	0.7	51.44	2838.8	213.8	2549.6	2838.8	6.5	2.6	2711.9
3.2	8	0.7	58.52	2838.8	213.8	2549.6	2838.8	6.9	2.7	2704.8

Column 4 is calculated by Equation 2.23, Column 5 is calculated by Equation 2.21 Column 6 is calculated by Equation 3.3, Column 7 is calculated by Equation 3.4, Column 8 is calculated by Equation 3.5, Column 9 is calculated by 2.24, column 10 is calculated by 2.30, and column 11 is subtraction of column 6, 7 and 8 by column 4 and 5.

As shown in the Figure3.2, the e/D ratio is between 0.1 and 1.0 does not change the ratio between In-line forces and lift forces therefore refereeing to reference [5], the effect of occurrence of lift forces start in e/D = 0.1 and this value will be accepted as valid condition in all calculation in this thesis.

Keeping e/D = 0.1 the changes in In-line forces and lift forces is again compared in order to observe the effect of wave height on Hydrodynamic forces. Figure 3.3 shows that at all depths any increase in wave height linearly decreases the ratio between total inline forces and lift forces. This ratio however increases as the depth increases, since the increase in the wave height maximum the effect the orbital velocity one can calculate that the effect of magnitude of orbital velocity is more dominate in the calculation of lift forces.

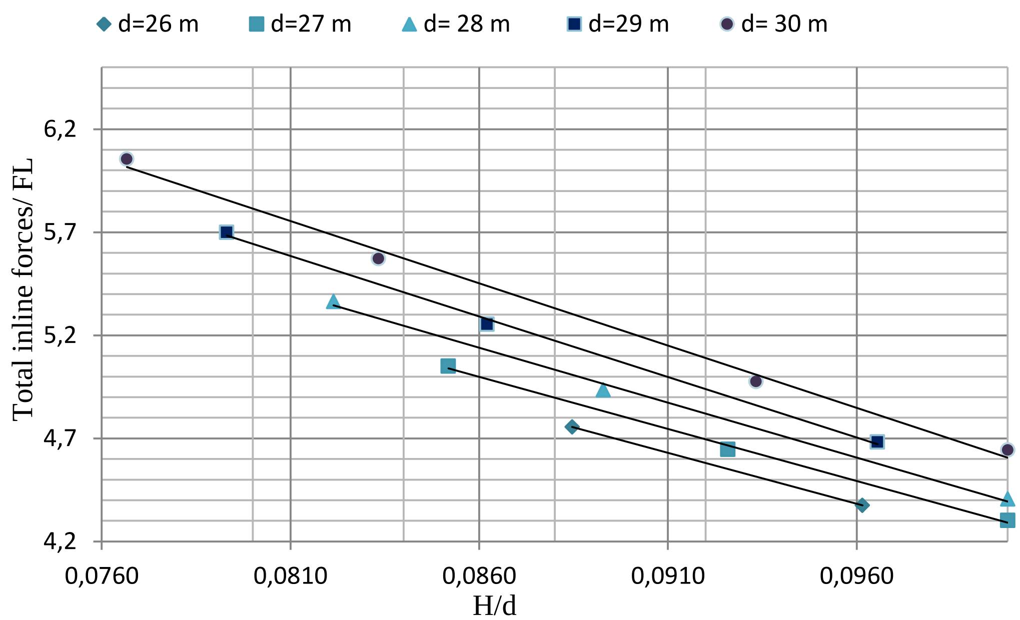

Figure 3.3: Comparison of in- line forces to lift forces at the different wave heights and depths.

Similar results can be depicted when the diameters of the submerged is under consideration. H is clear from Figure 3.4 that at constant depths and diameters, as the wave height increases the ratio of total In-line forces to lift forces decreases proving that the orbital velocity is more effective on lift forces than In-line forces. On the other hand as the H/D ratio is kept constant as the depth increases In-line forces becomes dominate with respect to the lift force.

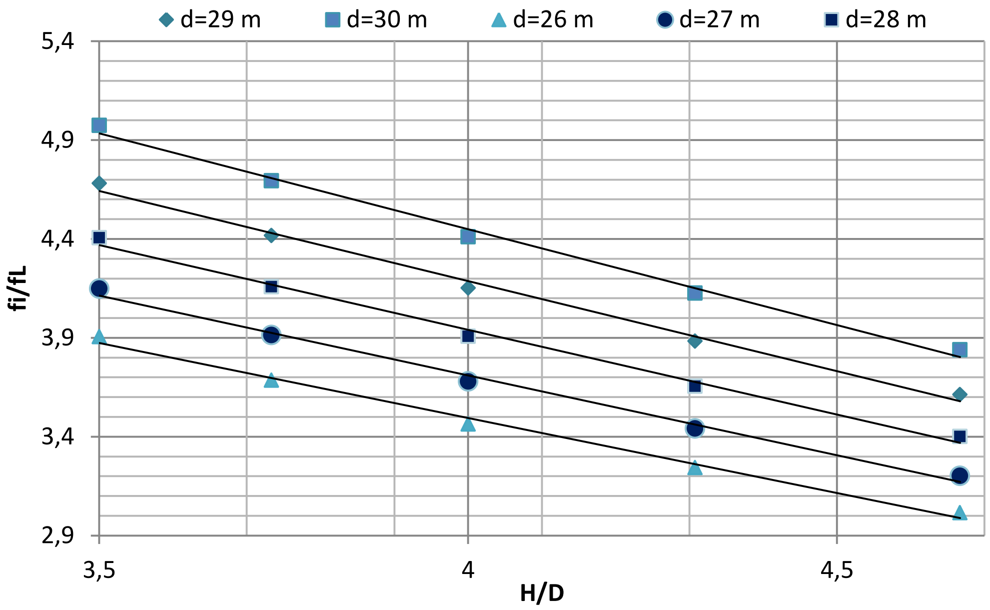

Figure 3.4: Linear relationship between dimensionless force ratio and wave height to pipe diameter ratio.

3.3 Summary of the chapter

In this chapter the inline and cross-line forces acting on submerged pipes at intermediate depths are calculated. The magnitudes of cross line forces were more than inline forces. The main reason of this was decreasing effects of orbital velocity at studied depths. Next chapter will help to evaluate the effects of cross-line forces in terms of spanning lengths.

Chapter 4

Spanning length analyses and comparison

4.1 Overview

This chapter will present the effects of hydrodynamic forces on offshore free span pipes and analyze the critical spanning lengths before failure. The failure is accepted to occur when the pipe yielding stress is exceeded. There are lots of submerged pipelines caring potable water, oil and gas etc, from one location to another. The impact of currents and waves on such pipelines is of main concern especially when the stability criteria changes due to settlements or scouring of the bottom of the pipes. Few researches has been reported about the effect of these waves and currents on submerged pipeline stability when HDPE pipes are under concern and when the Keulegan-Carpenter number is between 4 and 7.

4.2 Free span length based on allowable yield stress

An allowable yield stress method is used to find out the limits of suspension of free spanning pipes. In this method the allowable yield stress formulas for a simple supported beam is used to determine the maximum spanning length of submerged pipe. The results for different diameters and thicknesses are analyzed and general solutions are proposed by derived Figures.

4.2.1 Bending of pipes with both ends simply supported and under distributed load

In general bending or flexure is the behavior of a slender structural element subjected to an external load applied perpendicularly to a longitudinal axis of the element. In a simply supported beam, the distributed or concentrated loads applied to the pipe will create bending moment across the beam. These bending moments can lead the beam to deflect which is named bending deflection [26]. Figure 4.1 shows t a slandering pipe which is under the effect of uniformly distributed vertical forces. The shear force diagram and bending moment diagrams of the pipe are also given in Figure 4.1.

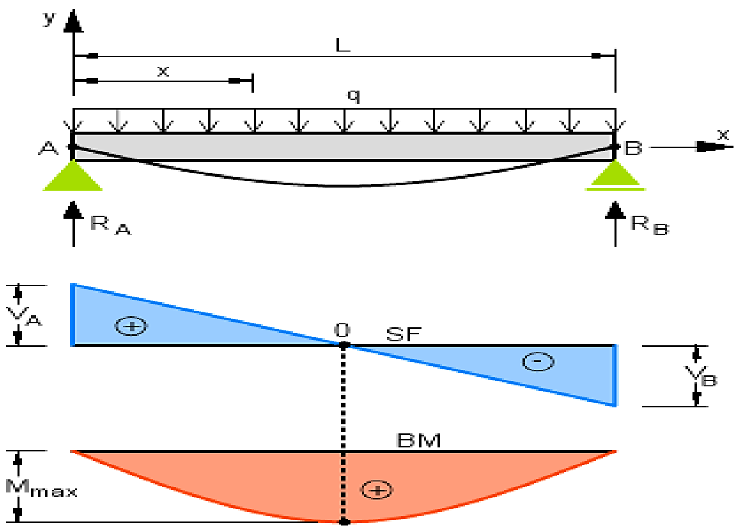

Figure 4.1:Apipe under uniform, distributed load and its shear force and bending moment diagrams

As is shown in the Figure 4.1, the maximum bending moment occur at the center of the pipe where the shear forces are balancing. The equation of the maximum moment can be easily obtained by dividing the pipe into several sections and writing the moment equations of each section. Anyhow, it is very well known and can be directly obtained from any structure book that the maximum moment for simply supported pipe is defined as

$$M_{\max} = \frac{qL^2}{8} \tag{4.1}$$

In which q is the net cross line forces per unit length and L is the length of the slender pipe. The maximum moment is necessary since it helps to find out whether the stresses occurring at the center exceeds the yield stress of pipe or not. The general equation for determining the bending stress for a slender pipe at any kind of boundary conditions is

$$S = \frac{MY}{I} \tag{4.2}$$

Where S is the bending stress, Y is the perpendicular distance to the neutral axis, I is the second moment of area about the neutral axis and M is bending moment at the point where the stress is in question. For simple supported pipes the maximum moment is experienced at the center of the length of the pipe. As long as the maximum moment due to the cross line forces is calculated the magnitude of bending stress can be predicted by using Equation (4.2). By comparing the yield stress with bending stress of the pipes, critical spanning length, Lp, can be easily put out as following in below:

$$L_P = \sqrt{\frac{8SI}{qY}} \tag{4.3}$$

In which s is equal to yield stress of the pipe and Y is the perpendicular distance to the neutral axis at the center of pipe, it means that Y=D/2.

The spanning lengths of pipes for different diameters and pipe thicknesses are calculated and are summarized in Table 4.1.

Table 4.1: Free span length based on allowable yield stress with simple supports at both ends

D_0 (m)	t (m)	D_I (m)	F_y (N/m^2)	W of pipe (N)	W of Content (N)	Wof Added Mass (N)	Total weight (N)	F_L (N)	F_B (N)	Net Force (N)	I (m^4)	L_P (m)
0.8	0.059	0.68	2.50E+07	1288.8	3586.1	5046.8	9921.7	70.6	514.46	4804.26	9.46E-03	31.4
0.8	0.047	0.70	2.50E+07	1054.9	3829.7	5046.8	9931.4	70.6	514.46	4814.01	7.96E-03	28.8
0.8	0.038	0.72	2.50E+07	858.4	4034.4	5046.8	9939.6	70.6	514.46	4822.20	6.63E-03	26.2
0.8	0.025	0.75	2.50E+07	561.8	4343.3	5046.8	9952.0	70.6	514.46	4834.55	4.49E-03	21.6
0.8	0.02	0.76	2.50E+07	452.3	4457.4	5046.8	9956.5	70.6	514.46	4839.12	3.66E-03	19.5
0.8	0.016	0.76	2.50E+07	364.1	4549.2	5046.8	9960.2	70.6	5046.8	4842.79	2.97E-03	17.5
0.7	0.065	0.57	2.50E+07	1212.1	2510.8	3864.0	7586.9	78	393.88	3653.75	6.56E-03	29.6
0.7	0.042	0.61	2.50E+07	819.1	2920.2	3864.0	7603.3	78	393.88	3661.29	4.72E-03	27.2
0.7	0.034	0.63	2.50E+07	667.7	3077.9	3864.0	7609.6	78	393.88	3667.59	3.94E-03	24.8
0.7	0.027	0.64	2.50E+07	541.2	3209.7	3864.0	7614.8	78	393.88	3672.87	3.26E-03	22.5
0.7	0.017	0.66	2.50E+07	351.2	3407.6	3864.0	7622.8	78	393.88	3680.78	2.17E-03	18.4
0.7	0.013	0.67	2.50E+07	276.0	3485.9	3864.0	7625.9	78	3864.0	3683.91	1.73E-03	16.4
0.6	0.046	0.50	2.50E+07	758.1	1982.6	2838.8	5579.6	65.1	289.38	2675.62	3.11E-03	27.8
0.6	0.036	0.52	2.50E+07	595.7	2151.8	2838.8	5586.3	65.1	289.38	2682.38	2.53E-03	25.1
0.6	0.029	0.54	2.50E+07	484.9	2267.2	2838.8	5590.9	65.1	289.38	2687.00	2.11E-03	22.9
0.6	0.024	0.55	2.50E+07	410.4	2344.8	2838.8	5594.0	65.1	289.38	2690.10	1.81E-03	21.2
0.6	0.019	0.56	2.50E+07	331.4	2427.1	2838.8	5597.3	65.1	289.38	2693.40	1.49E-03	19.2
0.6	0.012	0.57	2.50E+07	213.18	2549.6	2838.8	5602.2	65.1	2838.8	2698.30	9.8E-04	15.6

Column 5 is calculated by Equation 3.3, Column 6 is calculated by Equation 3.4 Column 7 is calculated by Equation 3.5, Column 8 is calculated by summation of column 5, 6 and 7, Column 9 is calculated by Equation 2.23, Column 10 is calculated by 2.21, column 11 is calculated by subtraction of column 8 with summation of column 9 and 10, and column 12 is calculated by Table 4.2, column 13 calculated by (4.2).

It is evident from Figure 4.2 that at constant diameters, as the internal diameters decreases the free spanning pipe increases. On the other hand as kept the diameter, thicknesses have a direct relationship with free spanning pipes.

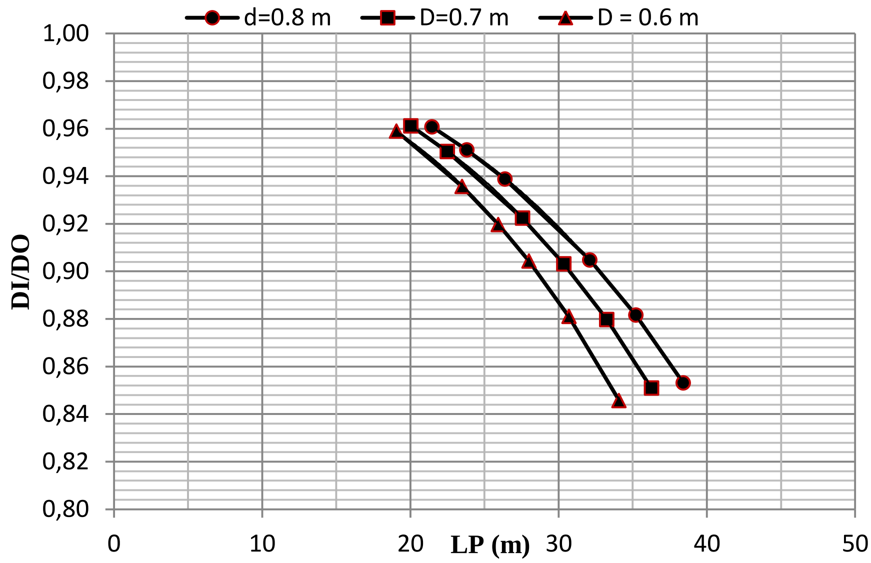

Figure 4.2: Ratio between free span pipes to internal diameter over outer diameter

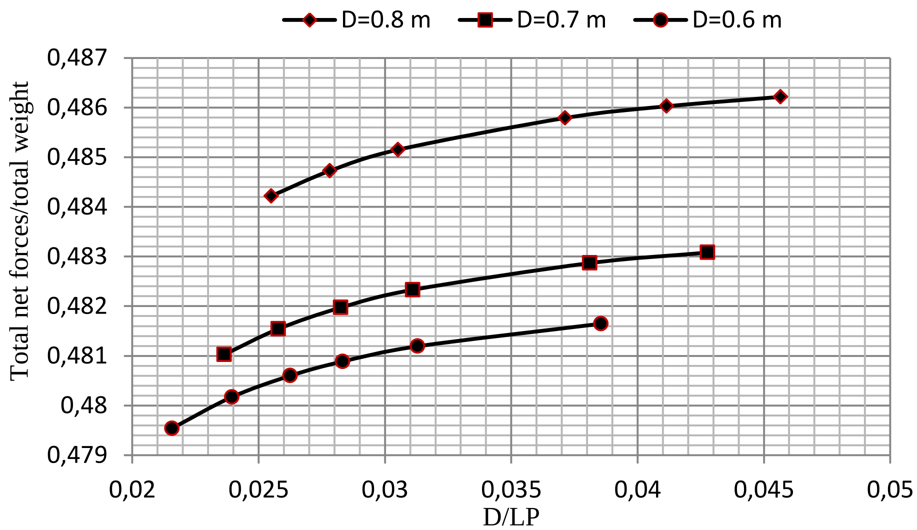

Figure 4.3: Relationship between dimensionless force ratio on total weight and diameter on free span length ratio.

4.2.2 Material properties of HDPE pipes

Table 4.2 illustrates material specifications and properties belonging to modelled pipe. The data for modulus of elasticity, poison ratio and yield stress are taken from ISO 178 [23] and DIN 53499 codes [24].

Table 4.2: Pipe Input Parameters

Input Parameters	Symbol	Magnitude	Unit
Outer pipe Diameter	D	0.8, 0.7, 0.6	(m)
Wall Thickness	Different thicknesses from ISO HDPE standard size and dimension		
Pipe Material	High density polyethylene – PE 100		
HDPE Density	P_{hdpe}	960	Kg/m^3
Young's Modulus	E	1.2*10^9	Pa
Poisson's Ratio	ν_{hdpe}	0.42	---
Plastic Section Modulus	Z_p	$\frac{\pi}{32D.}(D_0^4 - D_I^4)$	
Yield Stress	F_Y	2.5*10^7	N/m^2
Moment of Inertia	I	$\frac{\pi}{64}(D_0^4 - D_I^4)$	
Safety Factor	C	1.25	---
HDPE pipe Supports Types	Simply supports at both ends		

Since HDPE pipes are composite materials, the properties of products are usually showing differences from factory to factory or from project to project. In order to generalize the material properties the information given by standards and codes are preferred in this study.

4.2.3 Checks for vortex induced vibration in cross-flow directions

Even though the assumptions of $4<KC<7$ and Reynolds number smaller than 3.5×10^5 are thoroughly check throughout the analysis, vortex shedding criteria in the cross flow directions is re-evaluated.

The assessment of vortex shedding in cross flow direction is carried out through Table 4.3. Vortex shedding in cross-flow direction is delineated via comparing natural frequency and reduced velocity of flow by the help of Figure (2.7). The data calculated in Table 4.3 are then exported to the Figure (2.7) where the probability of occurrence of vortex induced vibration in cross flow direction is investigated and is presented as YES and NO.

Table 4.3: Assessment of vortex shedding in cross-flow direction

D_0 (m)	L_P (m)	u_{max} (m/s)	E (N/m^2)	I (m^4)	m_T kg	f_n HZ	Re	V_r	Figure (2.7)
0.80	31.37	0.50	1.20E+09	9.46E-03	1011.38	0.17	3.5*10	3.70	NO
0.80	28.76	0.50	1.20E+09	7.96E-03	1012.38	0.18	3.5*10	3.39	NO
0.80	26.22	0.50	1.20E+09	6.63E-03	1013.21	0.20	3.5*10	3.09	NO
0.80	21.55	0.50	1.20E+09	4.49E-03	1014.47	0.25	3.5*10	2.54	NO
0.80	19.44	0.50	1.20E+09	3.66E-03	1014.94	0.27	3.5*10	2.29	NO
0.80	17.52	0.50	1.20E+09	2.97E-03	1015.31	0.30	3.5*10	2.06	NO
D_0 (m)	L_P (m)	u_{max} (m/s)	E (N/m^2)	I (m^4)	m_T kg	f_n HZ	Re	V_r	Figure (2.7)
0.70	29.61	0.55	1.20E+09	5.61E-03	773.383	0.17	3.5*10	4.70	NO
0.70	27.16	0.55	1.20E+09	4.72E-03	775.053	0.18	3.5*10	4.31	NO
0.70	24.78	0.55	1.20E+09	3.94E-03	775.695	0.20	3.5*10	3.94	NO
0.70	22.51	0.55	1.20E+09	3.26E-03	776.233	0.22	3.5*10	3.57	NO
0.70	18.37	0.55	1.20E+09	2.17E-03	777.04	0.27	3.5*10	2.91	NO
0.70	16.37	0.55	1.20E+09	1.73E-03	777.359	0.30	3.5*10	2.60	NO

D_0 (m)	L_P (m)	u_{max} (m/s)	E (N/m^2)	I (m^4)	m_T kg	f_n HZ	Re	V_r	Figure (2.7)
0.60	27.82	0.52	1.20E+09	3.11E-03	568.762	0.16	3.5*10	5.28	NO
0.60	25.07	0.52	1.20E+09	2.53E-03	569.452	0.18	3.5*10	4.75	NO
0.60	22.86	0.52	1.20E+09	2.11E-03	569.923	0.20	3.5*10	4.33	NO
0.60	21.18	0.52	1.20E+09	1.81E-03	570.239	0.22	3.5*10	4.01	NO
0.60	19.17	0.52	1.20E+09	1.49E-03	570.575	0.24	3.5*10	3.63	NO
0.60	15.56	0.52	1.20E+09	9.80E-04	571.074	0.29	3.5*10	2.94	NO

Column 2 is calculated by Equation 4.2. Column 3 is calculated by Tables 3.1, 3.2 and 3.3, Column 5 is calculated by Table 4.2. Column 6 is calculated by summation of Equations 3.3, 3.4, and 3.5.Column 7 is calculated by Equation 2.27. Column 8 is calculated by 2.30, column 9 is calculated by 2.29.

4.2.4 Validation of results with previously given formulization.

The critical span length or the unsupported pipeline length at which oscillations of the pipeline occur for a specific current is based on the relationship between the natural frequency of the pipe free span and the reduced velocity. The critical span length for cross flow motion in literature is directly defined by the following equation

$$L_p = \sqrt{\frac{C\, V_r D}{2\pi U}\sqrt{\frac{EI}{M_e}}} \tag{4.4}$$

In which C represents a constant depending on the type of supports, M_e is the effective mass including the effect of added mass, V_r is the reduced velocity, U is the design velocity and D is the diameter of the pipe, [32]. The critical span length derived by Equation 4.4 and the span length derived in this thesis are given in Table 4.4. Figure 4.2 on the other hand shows the close relationship between the results of yield stress analysis and the Equation (4.3).

Table 4.4: Free span length based on allowable vortex shedding

D m	T m	D m	E N/m^2	I m^4	Mt kg	U_{max} m/s	Ur (cross) m/s	Re	C	L cross m
0.8	0.059	0.6824	1.20E+09	9.46E-03	1011.38	0.5	4.8	3.50E+05	1.57	35.74
0.8	0.047	0.7052	1.20E+09	7.96E-03	1012.38	0.5	4.8	3.50E+05	1.57	34.23
0.8	0.038	0.7238	1.20E+09	6.63E-03	1013.21	0.5	4.8	3.50E+05	1.57	32.69
0.8	0.025	0.751	1.20E+09	4.49E-03	1014.47	0.5	4.8	3.50E+05	1.57	29.64
0.8	0.02	0.7608	1.20E+09	3.66E-03	1014.94	0.5	4.8	3.50E+05	1.57	28.16
0.8	0.016	0.7686	1.20E+09	2.97E-03	1015.31	0.5	4.8	3.50E+05	1.57	26.74
0.7	0.052	0.5956	1.20E+09	5.61E-03	773.38	0.55	4.8	3.50E+05	1.57	29.91
0.7	0.042	0.6158	1.20E+09	4.72E-03	775.05	0.55	4.8	3.50E+05	1.57	28.64
0.7	0.034	0.6322	1.20E+09	3.94E-03	775.70	0.55	4.8	3.50E+05	1.57	27.37
0.7	0.027	0.6456	1.20E+09	3.26E-03	776.23	0.55	4.8	3.50E+05	1.57	26.09
0.7	0.017	0.6652	1.20E+09	2.17E-03	777.04	0.55	4.8	3.50E+05	1.57	23.57
0.7	0.014	0.6728	1.20E+09	1.73E-03	777.36	0.55	4.8	3.50E+05	1.57	22.25
0.6	0.046	0.5074	1.20E+09	3.11E-03	568.76	0.52	4.8	3.50E+05	1.57	26.53
0.6	0.036	0.5286	1.20E+09	2.53E-03	569.45	0.52	4.8	3.50E+05	1.57	25.19
0.6	0.029	0.5426	1.20E+09	2.11E-03	569.92	0.52	4.8	3.50E+05	1.57	24.06
0.6	0.024	0.5518	1.20E+09	1.81E-03	570.24	0.52	4.8	3.50E+05	1.57	23.17
0.6	0.019	0.5614	1.20E+09	1.49E-03	570.57	0.52	4.8	3.50E+05	1.57	22.04
0.6	0.012	0.5754	1.20E+09	9.80E-04	571.07	0.52	4.8	3.50E+05	1.57	19.87

The change in between the two different spanning length calculation can be formulated by

$$change\% = \left(1 - \frac{L_{P(Eq4.3)}}{L_{P(Eq4.4)}}\right) \times 100 \tag{4.5}$$

The percent change in the result is because of the reduced velocity variable given in equation 4.4. Since this term is read from a Table which is only valid for steel pipes, The results of equation 4.3 are more than what it should be for HDPE pipes.

Table 4.5: Comparing the results of Free span length based on allowable yield stress with simple supports at both ends and the proposed Equation (4.3) [32]

D_0 (m)	**T** (m)	**D_I** (m)	**L_P Eq (4.3)** (m)	**L_P Eq(4.4)** (m)
0.8	0.059	0.68	31.4	35.7
0.8	0.047	0.70	28.8	34.2
0.8	0.038	0.72	26.2	32.7
0.8	0.025	0.75	21.6	29.6
0.8	0.02	0.76	19.5	28.2
0.8	0.016	0.76	17.5	26.7
0.7	0.065	0.57	29.6	29.9
0.7	0.042	0.61	27.2	28.6
0.7	0.034	0.63	24.8	27.4
0.7	0.027	0.64	22.5	26.1
0.7	0.017	0.66	18.4	23.6
0.7	0.013	0.67	16.4	22.3
0.6	0.046	0.50	27.8	26.5
0.6	0.036	0.52	25.1	25.2
0.6	0.029	0.54	22.9	24.1
0.6	0.024	0.55	21.2	23.2
0.6	0.019	0.56	19.2	22.0
0.6	0.012	0.57	15.6	19.9

4.3 Deflection of spanning pipes

For the distributed loading on a pipe with simple supports at both ends, the deflection at any point of the pipe is given as

$$y_X = \frac{qx}{24EI}\left(L^3 - 2x^2L + x^3\right) \tag{4.6}$$

In which E is Young's modulus or modulus of elasticity, I is the second moment of area or area moment and L is the pipe length. The modulus of elasticity is in fact the property of material under loading. The deflection in each pipe under the vertical loading can be easily calculated by the help of Equation (4.4). Table (4.5) summarizes the predicted deflections in each pipe under consideration of this study.

Table 4.6: Deflection results for simply supported pipes.

D_0 (m)	t (m)	D_I (m)	Net forces (N)	E (N/m^2)	I (m^4)	L_P (m)	y (m)
0.8	0.059	0.6824	4804.3	1.2E+09	9.46E-03	31.40	0.17
0.8	0.047	0.7052	4814.0	1.2E+09	7.96E-03	28.78	0.16
0.8	0.038	0.7238	4822.2	1.2E+09	6.63E-03	26.24	0.14
0.8	0.025	0.751	4834.6	1.2E+09	4.49E-03	21.56	0.12
0.8	0.02	0.7608	4839.1	1.2E+09	3.66E-03	19.46	0.11
0.8	0.016	0.7686	4842.8	1.2E+09	2.97E-03	17.54	0.10
0.7	0.065	0.571	3644.9	1.20E+09	6.56E-03	29.61	0.16
0.7	0.042	0.6158	3661.3	1.20E+09	4.72E-03	27.16	0.17
0.7	0.034	0.6322	3667.6	1.20E+09	3.94E-03	24.78	0.15
0.7	0.027	0.6456	3672.9	1.20E+09	3.26E-03	22.51	0.14
0.7	0.017	0.6652	3680.8	1.20E+09	2.17E-03	18.37	0.11
0.7	0.014	0.6728	3683.9	1.20E+09	1.73E-03	16.37	0.10
0.6	0.046	0.5074	2675.6	1.20E+09	3.11E-03	27.82	0.20
0.6	0.036	0.5286	2682.4	1.20E+09	2.53E-03	25.07	0.18
0.6	0.029	0.5426	2687.0	1.20E+09	2.11E-03	22.86	0.17
0.6	0.024	0.5518	2690.1	1.20E+09	1.81E-03	21.18	0.15
0.6	0.019	0.5614	2693.4	1.20E+09	1.49E-03	19.17	0.14
0.6	0.012	0.5754	2698.03	1.20E+09	9.80E-04	15.56	0.11

Column 4 is calculated by Table 4.1. Column 6 is calculated by Table 4.2. Column 7 is calculated by Equation 4.4.

4.3.1 Validation of deflections by the help of computational fluid dynamics.

The sample model considered in this section is modeled in ANSYS software. The calculated value of the span is used to model the problem and the deflection of the pipe is evaluated (Figure 4.4). The model is constrained at the end so that the end does not move under application of force. The total weight of the dead load plus weight of the working fluid is applied as distributed load.

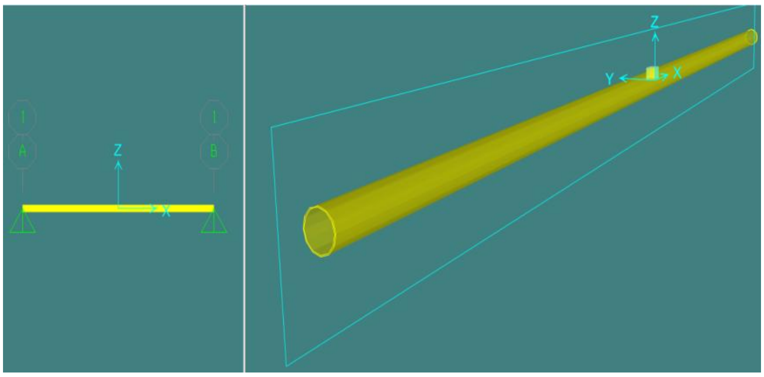

Figure 4.5: 3D view of the pipe modeling

In this study the simply support has been used at the both ends of pipe. It is evident that simply support pipes cannot have any movements at its support points, but no limit is placed on rotations at the supports. A series of pipes with different diameters were modeled by ANSYS regarding the standard diameters mention in DIN 1084 [10]. The aim is to calculate the deflections of spanning pipes for the maximum and minimum thicknesses. These results are then compared with the hand calculations of deflections of the pipes.

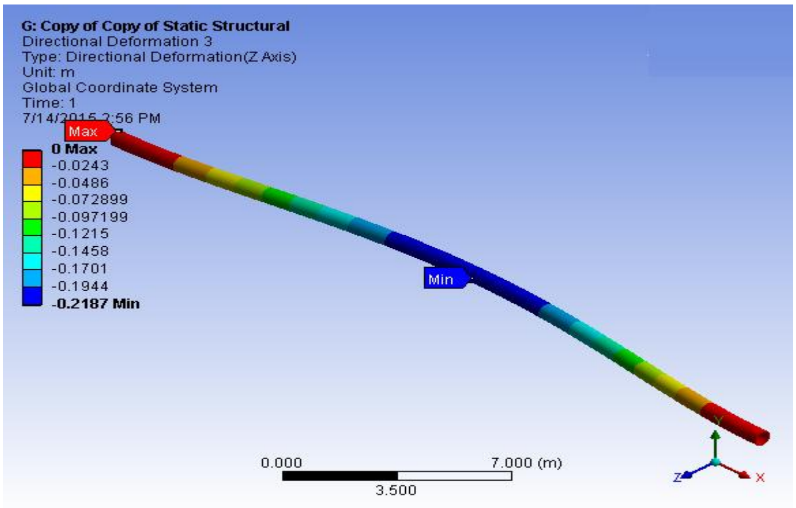

Figure 4.6: Deflection results of ANSYS for D=0.6 m.

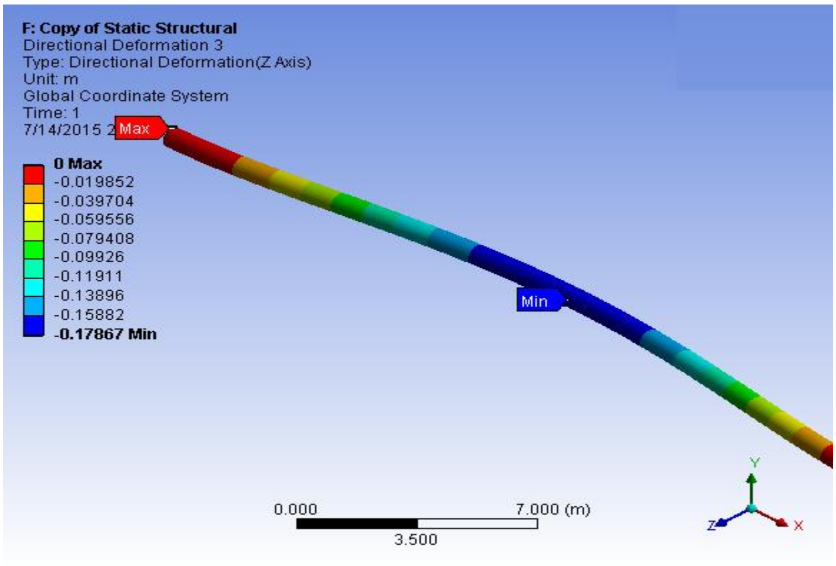

Figure 4.7: Deflection results of ANSYS for D=0.7 m.

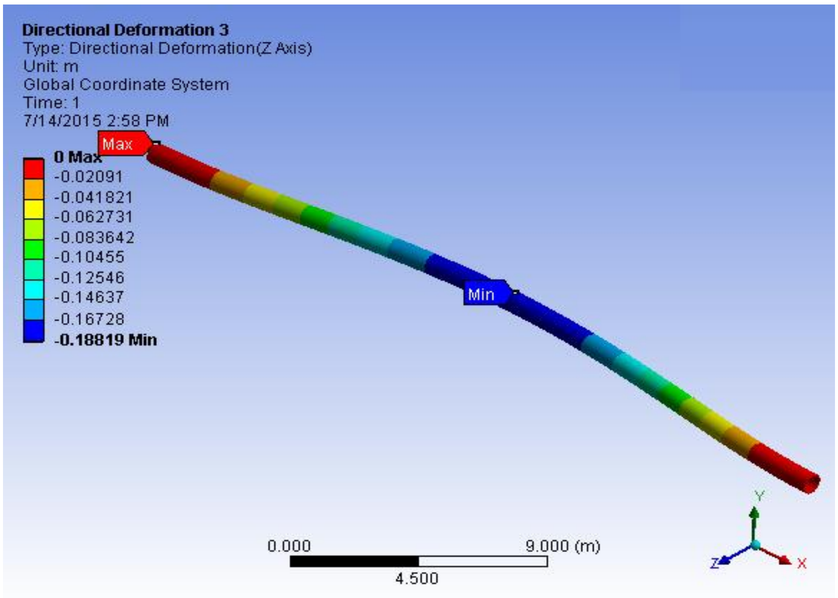

Figure 4.8: Deflection results of ANSYS for D=0.8 m.

The result of ANSYS has shown close relationship with the calculations carried out with Equation (4.4). The benefit of the Ansys solution was that one can easily observe the variation of deflection at any point along the pipes.

Chapter 5

Conclusion

5.1 Conclusion

This study has been carried out to calculate the maximum spanning lengths of different size HDPE pipelines at coastal environments. The work is limited to the low Reynolds number (less than 3.5×10^{5}) and Keulegan Carpenter number between 4 and 7. The limitations were valid at intermediate depths where the ratio of water depth to wave length is considered to be in between 0.05 and 0.5. Under these limitations all the hydrodynamic forces acting over the submerged cylindrical pipe at the bottom of the sea are deducted. Combinations of all the forces are sum up to two main forces acting at in-line and cross-flow directions. In addition, maximum free span lengths were calculated by using yield stress for three different diameters and variable thickness. The main conclusions of the study are as following:

- Until the e/D ratio is equivalent to 1, the magnitude of cross-flow forces is almost equal to the magnitude of in–line forces. As e/D ratio gets bigger the effect of cross-flow forces reduces and becomes negligible with respect to in-line forces when e/D becomes greater than 2.
- Whatever the depth of flow or the diameter of the pipe within the intermediate zone is; as the ocean wave height increases, the ratio between total inline force and lift force linearly decreases.

- The limitations of the study were assigned for preventing vortex induced vibration around the submerged pipes. The results of the study were all reviewed if this condition is satisfied or not. The outcomes show that the limitations are satisfactorily used with no vortex shedding vibration around the pipes.
- The maximum spanning length of the submerged HDPE pipes with simple supports at both ends are analyzed for their stability. The basic concepts of stability analyses were applied while the stress on the pipes due to the external forces was compared to the yield stress of HDPE pipes. This stability check was carried out for different diameter, different thickness and different lengths of the pipes.

5.2 Recommendations for Future Studies

The main aim of this study was to analyze maximum free span length of HDPE pipes when the limitation of KC between 4 and 7 were accepted. For future studies the author recommends to develop the analytical study by generating numerical analysis. Also, the behavior of the pipes can be further analyzed in the cases of different support systems like rigid supports. This study can be further developed by c analyzing the pipes at deep water depths while suspended in the sea. This will eliminate the effect of waves but dominate the effect of currents. Moreover, investigating the vortex induced shedding for in-line section and cross-flow section of suspended HDPE pipe when KC is bigger than 7 and finding maximum span lengths for different boundary conditions will be a positive achievement in offshore engineering.

REFRENCES

[1] Submarine pipeline systems, offshore standard DNV-OS-F101, Det Norske Veritas, October 2007, Norway

[2] Free spanning pipelines, recommended practice, DNV-RP-F105, Det Norske Veritas, 2006 Høvik, Norway

[3] BS 8010. (1993), Code of practice for pipeline-part 3. Pipeline subsea: Design, construction and installation, British.

[4]https://www.scribd.com/doc/7300254/DNV-Rules-for-Submarine-Pipeline-Systems-1981

[5] Sumer, B. M., & Fredsøe, J. (1997), *Hydrodynamics around cylindrical structures* (No. 12), World Scientific

[6] Mousselli, A. H. (1981). *Offshore pipeline design, analysis, and methods*.

[7] Kutz, M. (Ed.). (2011). *Applied plastics engineering handbook: processing and materials*. William Andrew.

[8] DNV (2010), "Recommended Practice DNV-RP-C205 Environmental Condition and Environmental Loads", Det Norske Veritas.

[9] Hsuan Y.G. and Timothy J. M., (1991). Pipe, H. D. P. E. NCHRP Report 429, National Academy press Washington, D.C.

[10] DIN 8074 Type 2, "Pipes of High-Density Polyethylene (High-Density PE), Type 2 Dimensions," 1980.

[11] ISO 12162 (1995) Thermoplastic materials for pipes and fittings for pressure applications – classification and designation – overall service (design) coefficient, Standard.

[12] Zang, Z. P., Teng, B., Bai, W., & Cheng, L. (2007). A finite volume solution of wave forces on submarine pipelines. *Ocean engineering*, *34*(14). 1955-1964.

[13] Ong, M. C., Utnes, T., Holmedal, L. E., Myrhaug, D., & Pettersen, B. (2010). *Numerical simulation of flow around a circular cylinder close to a flat seabed at high Reynolds numbers using a k–ε model*. Coastal Engineering, 57(10), 931-947.

[14] Choi, H. S. (2001). Free spanning analysis of offshore pipelines. *Ocean Engineering*, *28*(10), 1325-1338

[15] Toscano, R. G., Gonzalez, M., & Dvorkin, E. N. (2003). Experimental validation of a finite element model that simulates the collapse and post-collapse behavior of steel pipes. In Proceedings Second MIT Conference on Computational Fluid and Solid Mechanics.

[16] Water Wave Mechanics. Chapter II-1, Coastal Engineering Manual (EM 1110-2-1100) US Army Corps of Engineers, Washington, D.C. (2002).

[17] Patel, M. R. (2005). Wind and solar power systems: design, analysis, and operation. CRC press.

[18] Guo, B., Song, S., & Ghalambor, A. (2013). Offshore pipelines: design, installation, and maintenance. Gulf Professional Publishing.

[19] Journée, J. M. J., & Massie, W. W. (2000). *Offshore hydromechanics*.

[20] Det Norske Veritas (2008), Structural analysis of piping systems recommended *practice* DNV-RP-D101.

[21] Braestrup, M., Andersen, J. B., Andersen, L. W., Bryndum, M. B., & Nielsen, N. J. R. (2009). Design and installation of marine pipelines. John Wiley & Sons.

[22] https://www.scribd.com/doc/65441046/Chapter-1-History-Physical-Chemistry-Hdpe

[23] DIN EN ISO 178 Type 2, "*Plastics Determination of flexural properties), Type 2 Dimensions*," 2001.

[24] https://www.scribd.com/doc/116435365/DIN-53479

[25] DIN 8075-1987, "*High-Density Polyethylene (HDPE), General Quality Requirements Testing*," 1987

[26] Beer, F. P., Johnston Jr, E. R., Mazurek, D. F., Cornwell, P. J., Eisenberg, E. R., & Sanghi, S. (1962). *Vector mechanics for engineers* (Vol. 1). Tata McGraw-Hill Education.

[27] ANSYS Fluid User's Guide, Inc. Inc. Release 15.0, Southpointe November 2013 275 Technology Drive Canonsburg, PA 15317.

[28] American Society of Civil Engineers. (2007). *Seismic rehabilitation of existing buildings* (Vol. 41, No. 6). ASCE Publications

[29] Sollund, H. A., Vedeld, K., Hellesland, J., & Fyrileiv, O. (2014). *Dynamic response of multi-span offshore pipelines*. *Marine Structures*, *39*, 174-197.

[30] Zheng, Z. C., & Zhang, N. (2008). Frequency effects on lift and drag for flow past an oscillating cylinder. *Journal of Fluids and Structures*, *24*(3), 382-399.

[31] Yeganeh, B. A., Ghaheri, A., & Valipour, R. (2007). Analysis of offshore pipeline, allowable free span length.

[32] Guo, B., Song, S., & Ghalambor, A. (2013). *Offshore pipelines: design, installation, and maintenance*. Gulf Professional Publishing.

[33] Dalrymple, R. A., & Dean, R. G. (1991). *Water wave mechanics for engineers and scientists*. Prentice-Hall.

[34] Fox, R.W., Mconald, A.T..& Prichanrd, P.J., Fluid Mechanic,8th Edition, Wiley Publication. pg80.

Appendix A: MATLAB code

```
MATLAB CODE TO CALCULATE THE HYDRODYNAMIC FORCES
clear all;
clc;
eoverD = 2;
Cm = 35.729*eoverD^6 - 125.54*eoverD^5 + 177.12*eoverD^4
- 128.3*eoverD^3 + 50.691*eoverD^2 - 10.817*eoverD^1 +
2.202;
d =26;
pipediam = 0.8;
H = 2.3
T = 8.0;
Lo = 1.56 * T^2;
ratio = d/Lo;
if ratio < 0.5 & ratio > 0.0157
    else
    ratio = 0;
end

fprintf('ratio=')
fprintf('%8.2f\n',ratio)
     dratioL = 0.5;    x = 2*3.14*dratioL;
    delta = 0.01;
    K = 0;
    while abs(ratio - K)> delta
        x = 2*3.14*dratioL;
        K = dratioL * tanh(x);
        dratioL = dratioL - 0.01;
    end
fprintf('dratioL=')
fprintf('%8.2f\n',dratioL)

L = d / dratioL;
fprintf('L=')
fprintf('%8.2f\n',L)

DWCgo = 0.5 * T * 1.56;
WCg = 0.5 * (1 +
(4*3.14*dratioL/sinh(4*3.14*dratioL)))*(0.5*9.81*T*(1/3.1
4))*tanh(2*3.14*dratioL);
Ks = (DWCgo / WCg)^0.5;
fprintf('Ks=')
fprintf('%8.2f\n',Ks)


Hnew = Ks * H;
fprintf('Hnew=')
```

```
fprintf('%8.2f\n',Hnew)

zd = -1 * d + (pipediam / 2);
fprintf('zd=')
fprintf('%8.2f\n',zd)

t = [1:1:T];
for i = 1:T
gomma(i) = 2*pi*(zd + d)/L;
yomma(i) = (2*pi*d) / L;
alfa(i) = (9.81 * Hnew * T)/ (2*L) ;
beta(i)= cosh(gomma(i)) / cosh(yomma(i));
tattoo(i) = (-2*pi*t(i))/T;

u(i) = (alfa(i) * beta(i))* cos(tattoo(i));
uuu(i) = u(i) * ((zd + d)/d)^(1/7);
u(i) = u(i) + uuu(i);
end
fprintf('uuu=')
fprintf('%8.2f',uuu)
fprintf('\n')
fprintf('u=')
fprintf('%8.2f',u)
fprintf('\n')

t = [1:1:T];
    for i=1:T
gomma(i) = 2*pi*(zd+d)/L;
yomma(i) = (2*pi*d) / L;
alfa(i) = (9.81 * Hnew * T)/ (2*L) ;
beta(i)= cosh(gomma(i)) / cosh(yomma(i));
ua(i) = (alfa(i) * beta(i));
uuu(i) = ua(i) * ((zd + d)/d)^(1/7);
ua(i) = ua(i) + uuu(i);
KC(i) = ua(i)*T / pipediam;
    end

fprintf('ua=\n')
fprintf('%8.2f',ua)
fprintf('\n')
fprintf('KC=\n')
fprintf('%8.2f',KC)
fprintf('\n')

t = [1:1:T];
for i = 1:T
gomma(i) = 2*pi*(zd + d)/L;
yomma(i) = (2*pi*d) / L;
alfa(i) = (9.81 * Hnew * pi)/ (L) ;
beta(i)= cosh(gomma(i)) / cosh(yomma(i));
tattoo(i) = (-2*pi*t(i))/T;
```

```
a(i) = (alfa(i) * beta(i))* sin(tattoo(i));

end
fprintf('a=')
fprintf('%8.2f',a)
fprintf('\n')


Area = pi * pipediam * pipediam * 0.25;
dens = 1024; HydrodMass = 0;
for i=1:T

    HydrodMass(i) = Area * dens * Cm * a(i); end
            fprintf('HydrodMass = \n')
            fprintf('%8.2f',HydrodMass)
            fprintf('\n')


Area = pi * pipediam * pipediam * 0.25;
dens = 1024; KrylovF = 0;
for i = 1:T
   KrylovF(i) = Area * 1 * dens * a(i);
   end
fprintf('KrylovF = \n')
fprintf('%8.2f',KrylovF)
fprintf('\n')

RE = 0;
for i=1:T
    RE(i) = ua(i)* pipediam / (1.14 * 10^-6);
end
            fprintf('RE = \n')
            fprintf('%9.1d',RE)
            fprintf('\n')

if RE < 5*10^4
CD = 1.3;
end

if 5*10^4 < RE < 1*10^5
CD = 1.2;
end

if 1*10^5 < RE < 2.5 * 10^5
CD = 1.53 - (RE / 3 * 10^5);
end

if 2.5*10^5 < RE < 5*10^5
CD = 0.7;
else
CD = 0.7
```

```
end



fprintf('CD = \n')
   fprintf('%8.2f',CD)
   fprintf('\n')
dens = 1024;
DragF = 0;
for i = 1:T
    DragF(i) = 0.5 * dens * pipediam * CD * u(i)* u(i);
end
fprintf('DragF = \n')
fprintf('%8.2f',DragF)
fprintf('\n')

IlineF = 0;
for i = 1:T
    IlineF(i) = HydrodMass(i) + KrylovF(i) + DragF(i);
end
fprintf('IlineF = \n')
fprintf('%8.2f',IlineF)
fprintf('\n')


CL = 0.7;
dens = 1024;
LiftF = 0;
for i = 1:T
    LiftF(i) = 0.5 * dens * pipediam * CL * u(i)* u(i);
end
fprintf('LiftF = \n')
fprintf('%8.2f',LiftF)
fprintf('\n')
```